Nuclear Data Uncertainty Propagation for the Molten Salt Fast Reactor Design

Nuclear data uncertainty propagation for the Molten Salt Fast Reactor design

Nicolo' Abrate, Alex Aimetta, Sandra Dulla, and Nicola Pedroni

Politecnico di Torino, Dipartimento Energia, NEMO group
Corso Duca degli Abruzzi, 24 - 10129 Torino (Italy)

*Email: nicolo.abrate@polito.it

Number of pages: 41
Number of tables: 8
Number of figures: 18

Abstract

The development of new reactor technologies requires careful assessments of the various sources of epistemic uncertainties. In this work, the nuclear data uncertainties featuring the main isotopes of the U/Th MSFR design are propagated through Monte Carlo calculations to quantify the final uncertainty on some relevant integral parameters. In the first part of the paper, some best estimate calculations are performed by selecting different nuclear data libraries, showing the remarkable impact of this choice on the final responses. Then, the Generalised Perturbation Theory (GPT) routine available in Serpent 2 is adopted for a preliminary sensitivity and uncertainty analyses with respect to k_{eff}, highlighting a significant discrepancy between the covariance of the JEFF-3.3 and ENDF/B-VIII.0 library. After the selection of a few relevant nuclides, namely ^{7}Li, ^{19}F, ^{232}Th and ^{233}U, the Total Monte Carlo (TMC) method and the Unscented Transform (UT) are then adopted to estimate the uncertainty of other responses of interest like the Conversion Ratio and some multi-group constant. Some potential issues of the UT are highlighted and a mitigation strategy is applied. A relevant result of this analysis concerns the need for better data evaluations for the nuclides constituting the circulating salt for an effective deployment of the MSFR technology.

Keywords — Molten salt fast reactor, SANDY, Uncertainty propagation, Generalised Perturbation Theory, Unscented Transform, Total Monte Carlo

I. INTRODUCTION

The effective deployment of safe-by-design Generation IV reactors [1] demands the integration of preliminary safety studies since the early stage of development of these systems. In this context, the quantification and the propagation of the uncertainties associated with the input data through the whole calculation chain are of paramount importance, both in the design and licensing stages. In the first case, the knowledge of the confidence intervals featuring the calculations is mandatory to verify that the design constraints and goals are satisfied. In the second, this knowledge is necessary to ensure that the reactor operates reliably within the required safety margins.

These evaluations are even more important for new concept designs such as the Molten Salt Fast Reactor (MSFR), which has been the objective of the European projects EVOL, SAMOFAR and SAMOSAFER. With respect to other Gen-IV concepts, e.g. the Lead Cooled Fast Reactor, the MSFR technology presents some unique features aiming at enhancing its safety and sustainability. The most peculiar one is certainly the adoption of a circulating, liquid fuel, which eliminates by design some severe accidents like the core melting. In addition to the usual coupling between neutronics and thermal-hydraulics due to the fuel temperature (Doppler) reactivity and coolant density reactivity feedback mechanisms, the neutronics is also strongly coupled to the fluid-mechanics, because of the motion of the fission fragments in the core primary circuit.

The intrinsic multi-physics behaviour of the MSFR, the adoption of a circulating fuel and the peculiar unstructured geometry make the legacy codes, usually adopted for both the design and licensing phase, inadequate for the analysis of this reactor. Therefore, many efforts have been recently devoted, in the frame of the European projects SAMOFAR and SAMOSAFER, to develop *ad hoc* computational packages, which have been numerically benchmarked [2]. These codes offer models featured by different complexities, according to their intended applications. For core design applications, low-order transport models (like diffusion or SP_N) are usually coupled to Computational Fluid-Dynamics (CFD) codes using the Boussinesq approximation, while, for design verification, high-fidelity models involving the Monte Carlo approach for the neutronics and a two-phase compressible model for the thermal-hydraulics are used [3].

Another peculiarity of the MSFR design with respect to other Gen-IV fast reactor concepts is the adoption of uncommon nuclides in the nuclear fission industry: according to the design considered, the fast neutron spectrum can be achieved using a salt based either on Chloride or

on Fluorine and Lithium. In the first case, the reactor employs a traditional $^{238}U/^{239}Pu$ cycle, while in the last one, which is the study case of this paper, a closed $^{232}Th/^{233}U$ cycle is adopted. The presence of "new" nuclides for which little or no operational experience is available makes the quantification and the propagation of the uncertainties affecting the raw nuclear data mandatory for the evaluation of the final uncertainty in the main design parameters.

The nuclear data libraries include incident neutron cross sections for many reaction types (e.g., elastic scattering, fission...), energy and angle emission distributions, neutron multiplicities, and fission yields [4]. Considering that the data for each isotope depend at least on the incident neutron energy E and that the variable E spans several orders of magnitudes (from 10^{-11} up to 20 MeV), the overall number of uncertain parameters is huge. Due to the so-called *curse of dimensionality* [5], a brute-force exploration of the parameter space would not be computationally feasible even for the cheapest MSFR simulation tools, also considering that the nuclear data uncertainty is only one of the possible uncertainties affecting the reactor design and operation.

The task is usually simplified by propagating the nuclear data uncertainties to the set of few-group homogenised constants used in the low-order transport calculations. This reduces the dimensionality of the input parameter space from $10^4 \sim 10^5$ variables to about $10^0 \sim 10^2$ parameters, and allows to decouple the neutronic and the thermal-hydraulic calculations. Also due to its peculiar geometrical shape, the group constants featuring the MSFR are usually computed with Monte Carlo transport codes rather than with standard cell codes like the ECCO/ERANOS system [6]. Once the uncertainties are propagated to the group constants, some computationally smart techniques like the Polynomial Chaos Expansion (PCE) could be then used to propagate these uncertainties through the multi-physics calculations, thus mitigating the effects of the curse of dimensionality [7]. Even though, a full uncertainty propagation (UP) study involving only the neutronic calculations could be still computationally cumbersome. Since the number of uncertain input parameters is often much larger than the number of output parameters, a sensitivity analysis of the output with respect to the input variations is usually performed with perturbation methods like the Generalised Perturbation Theory (GPT). Then, first-order estimates of the response uncertainties may be obtained by the energy-dependent sensitivities [8]. Thanks to some recent advancements, most of the Monte Carlo transport codes available implement the GPT approach [9]. However, the memory requirements of the Monte Carlo GPT are proportional to the number

of input parameters and output responses, making its adoption for the group constants UP still difficult.

An alternative to perturbation methods is constituted by non-intrusive methods, which only require to sample the model a certain number of times. These methods have less memory requirements and are suitable for a large number of output responses, as in the case of group constants, but they may be computationally expensive to run if the number of model evaluations gets larger.

The most popular non-intrusive method is the Total Monte Carlo [10], which is very powerful since it allows to retrieve also the higher-order moments of the output distributions, although at the cost of hundreds/thousands model executions. Recently, some computationally cheaper alternatives to TMC have been proposed, like the Unscented Transform method (UT) [11], which allows to estimate the variance of the response with a reduced number of model evaluations. Despite this method has recently become quite popular in the nuclear data uncertainty propagation community [12–14], it seems that some important aspects concerning its application to Monte Carlo calculations have not been addressed yet in the literature for its effective deployment also in a stochastic simulation framework.

This paper has two main objectives. The first one is to carry out an uncertainty propagation study to investigate the impact of the nuclear data uncertainties related to the main isotopes in the MSFR on some relevant integral parameters, e.g. the effective multiplication parameter k_{eff}. The other one is to explore the application of alternative uncertainty propagation techniques to the GPT, like the TMC and the UT, which could be helpful in view of more complete uncertainty propagation studies focused on the group constants.

The paper is organised as follows. In section II the impact of some of the nuclear data libraries currently available is assessed on a set of best estimate calculations, showing how the choice of the library can affect the main integral parameters. Section III is devoted to presenting a brief review of the methods employed throughout the paper, i.e. GPT, TMC, and UT, while in section IV the results obtained with these methods are presented and discussed. Finally, some conclusions are drawn in section V, pointing out the necessity of improving the nuclear data for some nuclides for an effective deployment of the MSFR technology.

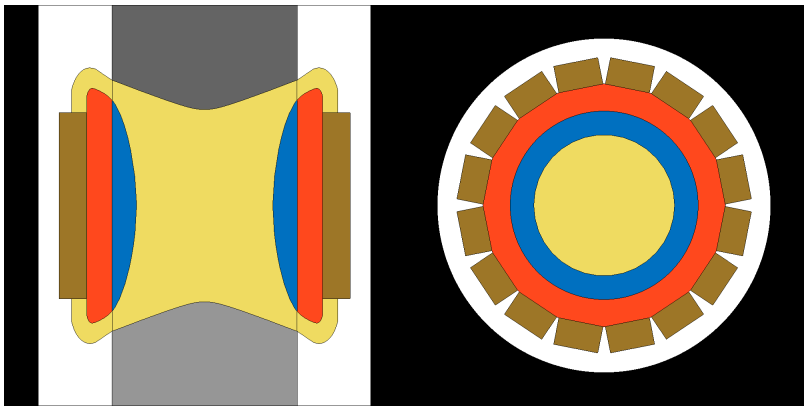

(a) *x-z plane* (b) *x-y plane*

Fig. 1. *Frontal (a) and upper (b) views of the MSFR 3D model implemented in Serpent. The fuel salt is represented in yellow, the breeding blanket in blue, the neutron shield in orange and the heat exchangers in gold. The dark and light grey regions are the upper and lower reflectors, respectively.*

II. BEST ESTIMATE SIMULATIONS WITH DIFFERENT NUCLEAR DATA LIBRARIES

Both design and licensing core calculations are generally performed using the best estimate data available in the nuclear data libraries. While the choice of the library should have a negligible impact on the final calculations for commercial reactors, the presence of uncommon nuclides like ^{19}F, ^{7}Li, ^{232}Th, and ^{233}U could make the choice of the library relevant for the MSFR design. Therefore, this section is devoted to presenting a set of best estimate Monte Carlo simulations carried out with different releases of two of the major nuclear data libraries, i.e. the ENDF and the JEFF projects.

The nominal calculations are run considering the 3D model of the MSFR sketched in fig. 1. The model was developed by the CIRTEN consortium in the framework of the European Projects EVOL and SAMOFAR, and is the same already adopted in a previous UP study on the MSFR [15]. The reactor is assumed to be at a uniform temperature of 900 K, which is roughly its average operating temperature. Each simulation is executed using the same calculation settings, i.e. 40 inactive and 100 active cycles, each with 10^6 neutrons, starting from an already converged fission source distribution, but changing each time the continuous-energy data library.

The calculations discussed in the following are performed with the releases ENDF/B-VII.1

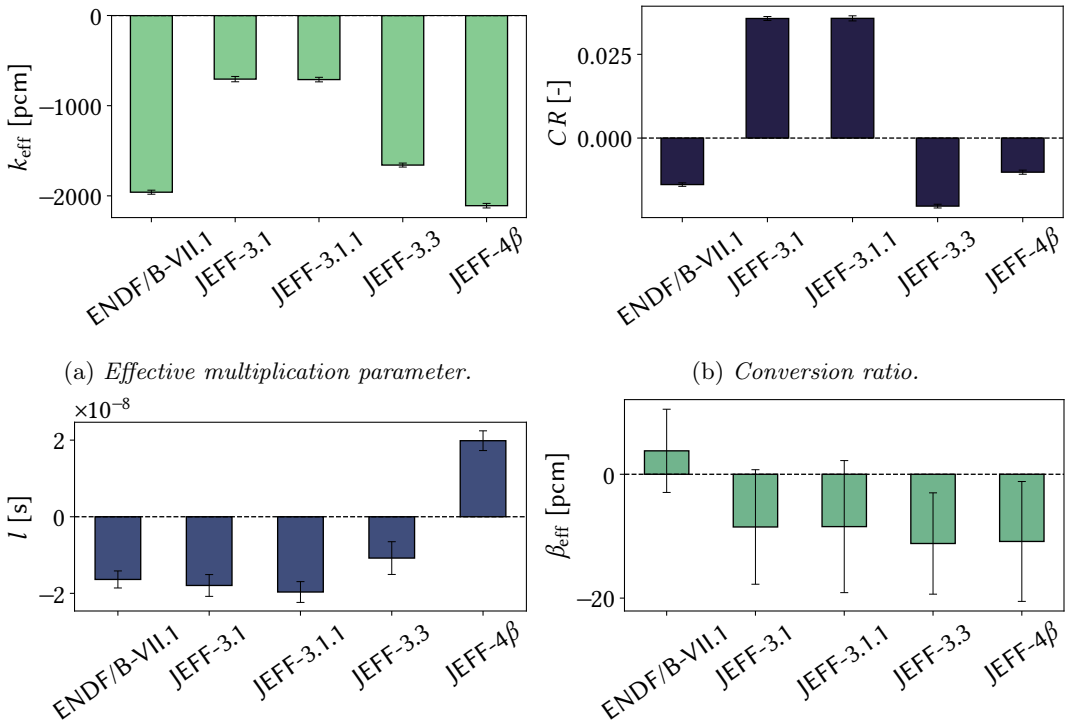

(a) *Effective multiplication parameter.*

(b) *Conversion ratio.*

(c) *Neutron lifetime*

(d) *Effective delayed neutron fraction.*

Fig. 2. *Difference between the reference values computed with the ENDF-B/VIII.0 and the ones computed with other libraries.*

and ENDF/B-VIII.0 of the ENDF project and with the releases JEFF-3.1, JEFF-3.1.1, JEFF-3.3, and the JEFF-4β of the JEFF project. The ENDF/B-VII.1, JEFF-3.1, and JEFF-3.1.1 libraries are the ones provided with the initial distribution of the Serpent 2 code, while the other ones, being more recent, have been processed from the ENDF-6 format to the ACE one with an in-house, open-source Python class, called NDL [16], which automatically invokes the NJOY tool [17, 18].

Figure 2 reports the difference between some integral parameters computed with the ENDF-B/VIII.0 library, which is assumed as a reference in this paper, and the ones computed with the other libraries previously mentioned. The largest differences can be observed for the effective multiplication parameter, where they can reach values around 2000 pcm. On the contrary, the discrepancies in β_{eff} are so tiny to fall within the statistical error of the Monte Carlo calculation, which is well below 20 pcm.

Figure 3 helps to understand the source of such large discrepancies in these integral param-

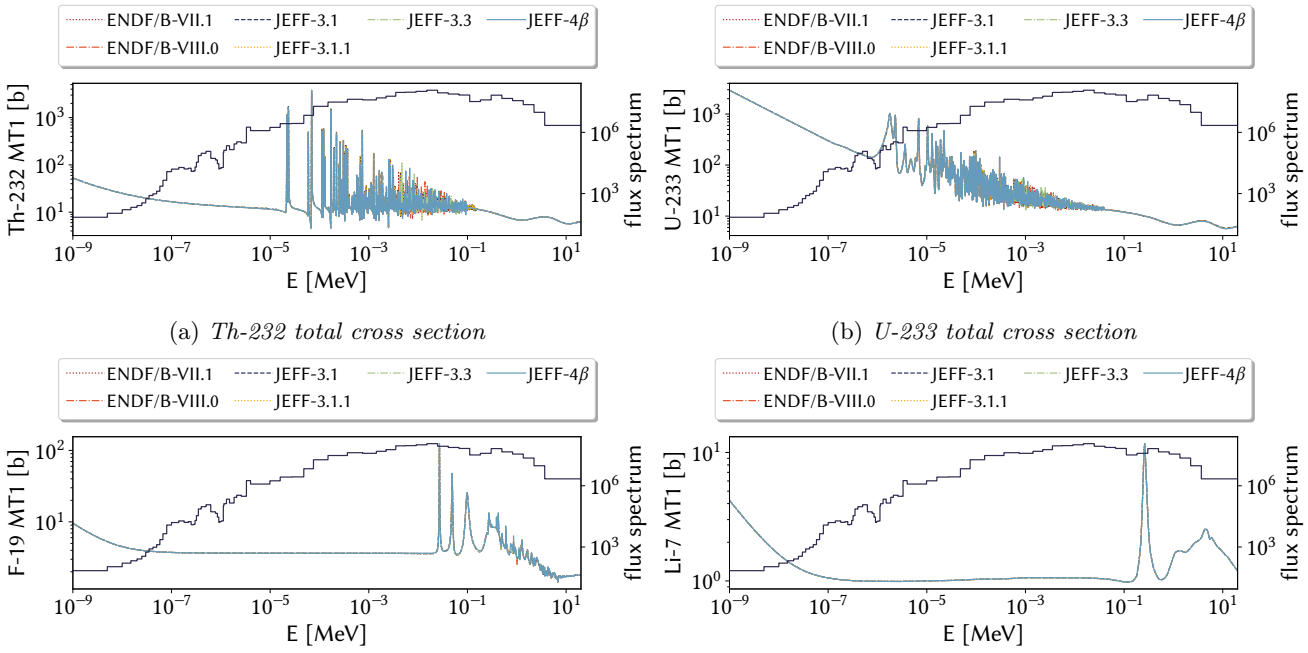

(a) *Th-232 total cross section*

(b) *U-233 total cross section*

(c) *F-19 total cross section*

(d) *Li-7 total cross section*

Fig. 3. *Different evaluations of the total cross section (MT1) for the main nuclides composing the fuel salt.*

eters, by showing the different total cross section evaluations for the isotopes composing the salt and its characteristic energy spectrum. Most of the discrepancies can be found in the resolved resonance region, above 10^{-4} MeV, where the flux is very large. Despite all these isotopes are not common in the nuclear industry, as one could expect, the nuclides featured by the largest discrepancies are the heavy ones, i.e. ^{232}Th, and ^{233}U, while the cross section of ^{19}F shows some significant differences around 1 MeV and the cross section of ^{7}Li does not exhibit relevant differences. Figure 4 provides an enlargement of the cross sections for ^{232}Th, ^{233}U and ^{19}F. Except for the JEFF-3.1 and JEFF-3.1.1 releases, all the libraries provide different values of the cross sections for the fissile isotopes, thus implying large differences also on k_{eff}.

The results presented in fig. 2 prove that the uncertainties associated with the cross sections of the main isotopes constituting the MSFR are extremely relevant, especially the ones impacting on k_{eff}, thus justifying the need for an uncertainty propagation study focused on the MSFR.

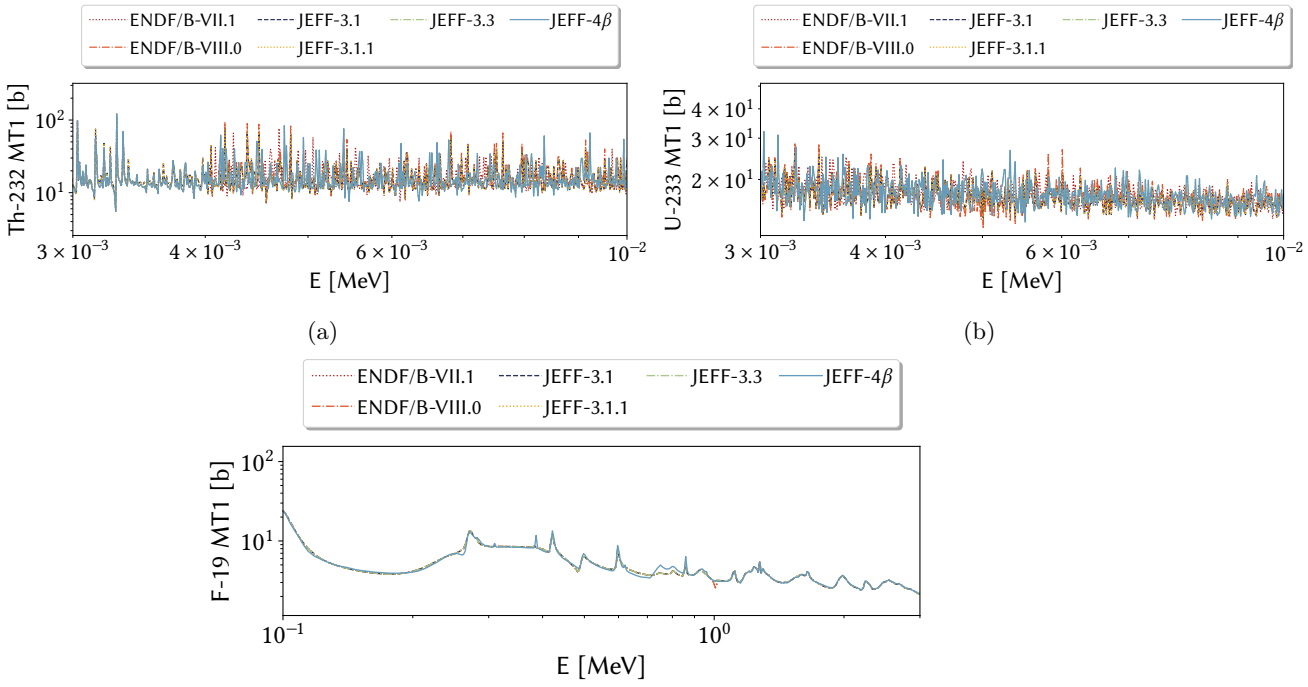

Fig. 4. *Enlargement of fig. 3 in the epithermal region.*

III. UNCERTAINTY PROPAGATION METHODS

This section aims at providing a concise review of the methods used for the uncertainty propagation study conducted in this paper. All the methods described in the following have been applied to Monte Carlo simulations of the MSFR, therefore a special focus will be given to the aspects pertaining to a stochastic simulation framework. Nevertheless, different applications of the same methods for deterministic calculations can be easily found in the literature as well.

III.A. Perturbation methods

Perturbation methods are widely employed in different fields of physics, especially for sensitivity analysis. The most popular perturbation approach in the physics of fission reactors is known as Generalised Perturbation Theory (GPT) [19, 20]. The neutron transport equation is a function of several input parameters, which are mostly cross sections, and can be adopted to estimate several responses, which are mostly reaction rates. In a single calculation, where an estimate of both solutions to the direct and adjoint transport equations is performed, the GPT allows to retrieve the

sensitivities of a set of arbitrary responses R_i, $i = 1, \ldots, I$ to a set of arbitrary input parameters P_j, $j = 1, \ldots, J$. As such, this approach is very convenient to estimate the variance of a certain response to a given input, by means of the *sandwich rule* [8],

$$\sigma_R^2 = \vec{\mathrm{S}}_P^r \mathrm{cov}[P] \vec{\mathrm{S}}_P^{R^T}, \tag{1}$$

where σ_R^2 is the response uncertainty, $\vec{\mathrm{S}}_P^R$ is the relative sensitivity of R to the input P, and $\mathrm{cov}[P]$ is the relative covariance matrix of P.

The input parameters depend on the neutron energy, therefore the same dependence affect both their covariance matrices and the sensitivity coefficients. This aspect points out a contradiction in the adoption of the Monte Carlo version of the GPT [9]: the Monte Carlo approach allows to describe the continuous-energy transport of neutrons but, at the same time, does not allow to estimate continuous-energy responses, due to the statistical noise. Hence, despite the transport process is simulated accurately, statistically significant sensitivities could be scored only on a limited number of energy groups. A possible solution to this contradiction is offered by the eXtended GPT (XGPT) technique, which amounts to approximate a continuous-energy covariance with a limited number of basis functions over which the continuous-energy sensitivities are projected [21].

Both these approaches, available in Serpent 2 and recently applied to perform sensitivity and uncertainty analysis in fast reactors [15, 22], are first-order accurate, being both based on eq. (1). In addition to the potentially limited accuracy of the sensitivities and, consequently, of the response variance, these methods can be quite memory consuming in a Monte Carlo framework. Moreover, it could be difficult to compute the sensitivities of bi-linear ratios, e.g., the β_{eff}, with sufficient precision due to the large number of latent neutron generations needed for the adjoint estimate [9, 21].

III.B. Non-intrusive methods

Most of the practical difficulties pertaining to perturbation methods could be solved relying on non-intrusive methods, which consider the model under investigation as a black-box communicating with the external world through inputs and outputs. As such, these methods do not demand any modification to the model, being thus very general, but rather focus on the input data given to the black-box. Sometimes, a simple brute-force technique may be adequate to map the behaviour

of the model, just feeding it with a set of random input parameters. In most of cases, however, computationally smarter methods are envisaged to carefully select a limited number of original model evaluations.

In the following, both these approaches will be examined for propagating the uncertainty through a Monte Carlo transport model. Being non-intrusive, they require a procedure to generate a set of perturbed nuclear data to map the system's behaviour. The cross sections perturbations are accomplished by using the open-source Python package SANDY [23]. This code offers an efficient Application Programming Interface (API) to interact with the ENDF-6 files. Exploiting the information on the best estimate data and their covariance, SANDY allows to sample the perturbed data according to a normal or log-normal distribution and finally dumps them into ENDF-6 files. Despite the SANDY API could be used to automatically process these raw files into the ACE format, requested by Serpent 2, with NJOY, the NDL Python package has been adopted in order to process the data more efficiently.

III.B.1. Total Monte Carlo

In the nuclear data community, the brute-force, direct sampling approach is known as Total Monte Carlo [10]. This methodology consists of generating a large set of perturbed nuclear data files and then running one Monte Carlo simulation for each sample. This procedure can be very computationally expensive, since its convergence trend scales as $1/\sqrt{N}$, where N is the number of samples. The resulting variance of the response R is a sum of two terms, namely

$$\sigma_R^2 = \sigma_{alea}^2 + \sigma_{epis}^2, \tag{2}$$

where σ_{alea}^2 is the *aleatoric* variance, associated with the statistical noise of each Monte Carlo simulation, and σ_{epis}^2 is the *epistemic* uncertainty due to the nuclear data.

The computational cost of each Monte Carlo simulation is in general weakly related to the number of output responses, making this approach adequate when the UP involves multiple responses. To overcome the cost of this method, faster alternatives have been proposed in the literature, like the fast TMC [24] and the method developed at the Gesellschaft für Anlagen- und Reaktorsicherheit company, known as GRS method [25]. These methods have been recently applied for the nuclear data uncertainty propagation in the frame of fusion reactors design [26]. In

this paper, however, only the TMC approach will be addressed, since it allows to estimate also the higher-order moments of the sample distribution. Being the most accurate method available, this method will be used in the following section to benchmark the results obtained with the other UP methods.

III.B.2. Unscented Transform

The basic principle of the Unscented Transform (UT) [11] is to estimate the first and second order moments of the responses distributions approximating the input distribution rather than the model. This idea is practically justified by the fact that approximating the input distribution is often easier than acting on the model, especially when it is non-linear.

The input approximation is achieved by generating a set of so-called *sigma points* that capture the essence of the input data distribution. When the goal of the analysis is the evaluation of the first two moments of the response distribution, $2k+1$ sigma points are sufficient to get a reliable representation of the input, where k corresponds to the dimensions of the input perturbed data. When dealing with nuclear data, k is equal to $n_{\mathrm{MT}}H$, where n_{MT} is the number of MT reaction channels considered for the nuclide under examination and H is the number of energy groups employed to score the covariance matrix. In case more than one isotope are considered, $k = n_{\mathrm{MT}}Hn_{\mathrm{ISO}}$, where n_{ISO} is the number of isotopes. Since k can become very large, suitable reduction techniques, like the one applying the Low Rank Approximation (LRA) to the Singular Value Decomposition (SVD) [27, 28], are often considered.

The elements constituting the vector of sigma points $\vec{\chi}$ are computed according to the following definitions [27]:

$$\begin{aligned} \chi^{[0]} &= \mu \\ \chi^{[i]} &= \mu + \left(\sqrt{(k+\lambda)\hat{C}}\right)_i \quad \text{for } i = 1, ..., k \\ \chi^{[i]} &= \mu - \left(\sqrt{(k+\lambda)\hat{C}}\right)_{i-k} \quad \text{for } i = k+1, ..., 2k, \end{aligned} \tag{3}$$

where $\hat{C} \in \mathbb{R}^{k\times k}$ is the covariance of the input, μ is the mean vector of the input (i.e. the nominal cross sections from the nuclear data library) and λ is an arbitrary spreading parameter

that influences the weights assigned to each sigma point,

$$\omega^{[0]} = \frac{\lambda}{k+\lambda} \tag{4}$$
$$\omega^{[i]} = \frac{1}{2(k+\lambda)} \quad i = 1, \ldots, 2k.$$

Hence, according to the application and the model, the spreading parameter should be carefully selected [29]. The sigma points are passed to the non-linear model $\mathcal{M}'$ to get a set of responses, which are then used to estimate the moments of the output distributions as a weighted mean and a weighted covariance, respectively:

$$\mu' = \sum_{i=0}^{2k} \omega^{[i]} \mathcal{M}'\left(\chi^{[i]}\right), \tag{5}$$

$$\hat{C}' = \sum_{i=0}^{2k} \omega^{[i]} \left(\mathcal{M}'\left(\chi^{[i]}\right) - \mu'\right) \left(\mathcal{M}'\left(\chi^{[i]}\right) - \mu'\right)^T, \tag{6}$$

where the index i corresponds to the *i-th* sigma point and weight.

When the covariance matrix is symmetric and positive semi-definite, the corresponding square root can be computed with the SVD,

$$\hat{C} = V \Sigma V^T, \tag{7}$$

where the matrix Σ is a diagonal matrix composed by the singular values (SV) of $\hat{C}$. Usually, the number of non-zero SV, say r, is lower than the rank of $\hat{C}$. When $\hat{C}$ is positive semi-definite, its square root can be computed as:

$$\sqrt{\hat{C}} = V \Sigma^{1/2}. \tag{8}$$

Due to some round-off errors occurring in the multi-group covariance extraction from the nuclear libraries, this matrix may be non-positive semi-definite. Thus, before the UT can be applied, the closest semi-positive definite matrix to the original one is evaluated employing the *statsmodels* Python package [30], following the procedure given in [31].

Since the singular values constitute a monotonically decreasing sequence which usually decays quite rapidly, the SVD factorisation can be truncated at the price of small approximations, moving from r SV to t, where the last symbol indicates the number of SV retained after the truncation.. Thanks to the strong correlation in the nuclear data, an effective truncation can be often applied

to reduce the dimensionality of the matrix.

Consequently, the truncation allows to decrease the number of sample points from $2k+1$ to $2t+1$ and, thus, the computational time of the uncertainty propagation. In fig. 5, a sketch of the SVD-UT algorithm followed in the paper is provided. From each ENDF file, the mean and the covariance information are obtained. The application of the SVD and LRA algorithms allows to extract a truncated square root of the covariance matrix, which is then employed to generate a specific set of perturbed cross sections, known as *sigma*-points (or σ-points) in the UT jargon. These data are then passed to the non-linear model, which produces a set of output responses used to estimate its mean and the covariance.

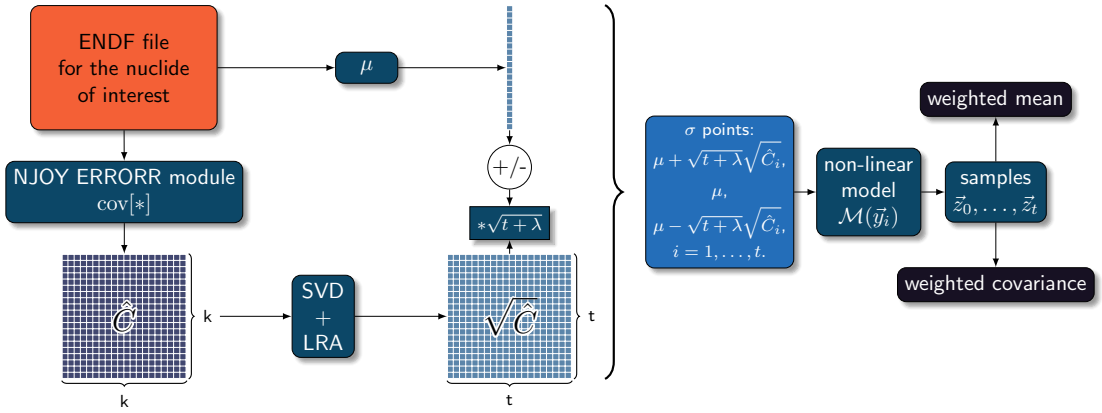

Fig. 5. *Schematic of the Unscented Transform method. The*

In this work, the sigma points are generated by perturbing the nuclear data with the SANDY API, applying a perturbation factor defined as:

$$p_{SP} = 1 \pm \sqrt{(t+\lambda)\hat{c}}, \tag{9}$$

where $\hat{c}$ is the relative covariance matrix. When the scaling factor $(t+\lambda)$ is large, perturbation factors outside the range [0,2] may be obtained. Since non-physical, negative factors could be obtained with the multi-variate normal sampling offered by SANDY, the code automatically truncates the perturbation, setting the factor to 0 when it is negative or to 2 if it is larger than this value, in order to maintain a certain symmetry in the perturbations. Therefore, also in the UT case, some sigma points could be modified by the code during the files perturbation, thus leading

to a further approximation of the final results.

In this respect, a possible solution is to employ a variant of the UT, called the General Constrained Sigma Point (GCSP) method [32]. This method allows to generate all the perturbing factors inside the range [0,2], independently on the choice of t and λ, with the lower and upper limits respectively defined as μ_L, which in this case corresponds to 0, and μ_R, which in this case corresponds to 2. The new sigma points are defined as:

$$\begin{aligned} \chi^{[0]} &= \mu \\ \chi^{[i]} &= \mu + d_i \left(\sqrt{\hat{C}}\right)_i \quad \text{for } i = 1, ..., t \\ \chi^{[i]} &= \mu - d_i \left(\sqrt{\hat{C}}\right)_{i-t} \quad \text{for } i = t+1, ..., 2t, \end{aligned} \tag{10}$$

where:

$$d_i = \min\left(\sqrt{(k+\lambda)}, d_{i1}, d_{i2}\right), \tag{11}$$

$$\begin{aligned} d_{i1} &= \min|\mu_U - \mu_j| / \left|\left(\sqrt{\hat{C}}\right)_{j,i}\right|, \\ d_{i2} &= \min|\mu_L - \mu_j| / \left|\left(\sqrt{\hat{C}}\right)_{j,i}\right|, \end{aligned} \tag{12}$$

where j and i indicate the j-th row and i-th column of the matrix. The new weights are computed as:

$$\begin{aligned} \omega^{[0]} &= \frac{1}{2d_i^2} \\ \omega^{[i]} &= 1 - \sum_{i=1}^{2t} \omega^{[i]} \quad \text{for } i = 1, ..., 2t. \end{aligned} \tag{13}$$

Both the standard UT and the GCSP method have been employed in this work, in order to asses the impact of the truncation of the perturbing factors when the standard UT is applied.

IV. RESULTS

In this section, the main outcomes of the UP study involving some relevant integral parameters of the MSFR will be discussed, comparing also the performances of the different methodologies adopted.

IV.A. Sensitivity and uncertainty analyses with GPT

In spite of its limited energy resolution, the Monte Carlo GPT is probably the method providing the richest physical information concerning the relationship between the nuclear data and the response of interest, allowing to highlight the most important source of uncertainties. Due to the large number of input parameters, the functional dependence of a general response R, e.g., a reaction rate, may be expressed as follows,

$$R = f(\Phi(\vec{r}, E, \vec{\Sigma}_{x,y}(\vec{r}, E)), \Phi^{\dagger}(\vec{r}, E, \vec{\Sigma}_{x,y}(\vec{r}, E)), \vec{\Sigma}_{x,y}(\vec{r}, E)), \tag{14}$$

where Φ and $\Phi^{\dagger}$ are the forward and adjoint fluxes and $\vec{\Sigma}_{x,y}$ indicates the set of cross sections for the various isotopes x and for the various reaction channels y, which determines the distribution of the adjoint and direct fluxes in the system. The sensitivity of R to a cross section P can be expressed as a sum of an indirect term, related to the flux and, possibly, adjoint variations induced by P, and of a direct term, related to the $\vec{\Sigma}_{x,y}$ dependence,

$$S_P^R = \frac{\partial R/R}{\partial P/P} = \frac{P}{R}\frac{\partial R}{\partial P} = \frac{P}{R}\left(\frac{\partial R}{\partial \Phi}\frac{\partial \Phi}{\partial P} + \frac{\partial R}{\partial \Phi^{\dagger}}\frac{\partial \Phi^{\dagger}}{\partial P} + \frac{\partial R}{\partial \vec{\Sigma}_{x,y}}\frac{\partial \vec{\Sigma}_{x,y}}{\partial P}\right). \tag{15}$$

Each variable in eq. (15) is a function defined on the phase space, making this dependence even more intricate. Nevertheless, GPT is extremely valuable to get an insight into the physics of the system, yielding the sensitivity coefficient of R for different energies, isotopes, reaction channels, and reactor regions.

The Serpent 2 computation of the sensitivities, which are evaluated by simulating the continuous-energy transport process but are scored on a multi-group structure for statistical reasons, was carried out using 10^6 neutrons per cycle, 40 inactive cycles and 10^3 active cycles, subdivided into a batch interval of 25 cycles in order to avoid possible correlations within the 15 latent generations

needed to estimate the adjoint. The relative sensitivities were scored with respect to each isotope in the MSFR, each reaction channel and each material region for the effective multiplication parameter k_{eff}, the effective delayed neutron fraction β_{eff}, the neutron lifetime l, and the void coefficient. The overall calculation took about 100 GB of RAM and required about 4.5 days on 24 CPUs on a cluster.

Despite the simulation being carried out with large computational resources, only the sensitivities for k_{eff} turn out to have an acceptable statistical error. The large statistical deviations in the sensitivities of the other integral parameters are probably a cause of their small values, as it will be shown in the following sections, meaning that these quantities are scarcely affected by uncertainties in the cross sections.

The output of the sensitivity calculation showed in the following figures was processed with the serpentTools python package [33]. Figures 6 and 7 show some examples of the multi-group sensitivities of k_{eff}, computed with the ENDF-B/VIII.0 library, and the relative variances of some reactions for some isotopes, taken from the nuclear data libraries JEFF-3.3, JEFF-4β and ENDF-B/VIII.0. Both sensitivities and variances are scored on the ECCO-33 group structure, which is a standard grid used for fast reactors analysis [22]. Most of the 33 groups featuring this grid are distributed in the epithermal and fast regions, while only one group is employed in the thermal region, between 10^{-7} and 10^{-11} MeV.

TABLE I
Description of the MT reaction numbers used throughout the paper.

MT	description
MT2	Elastic scattering
MT16	Production of two neutrons
MT18	Total fission
MT22	Production of a neutron and an α particle
MT102	Radiative capture
MT107	Production of an α particle

The physical meaning of each MT reaction used throughout the paper is reported in table I. Figure 6 reports the sensitivities to the elastic scattering (MT2) and radiative capture (MT102) reactions for ^{7}Li and ^{19}F. The sensitivity of k_{eff} to the elastic scattering is large and is featured by a larger statistical noise, which is probably due to the fact that perturbations in the elastic scattering affect the leakages and, consequently, the fission source distribution, as already observed

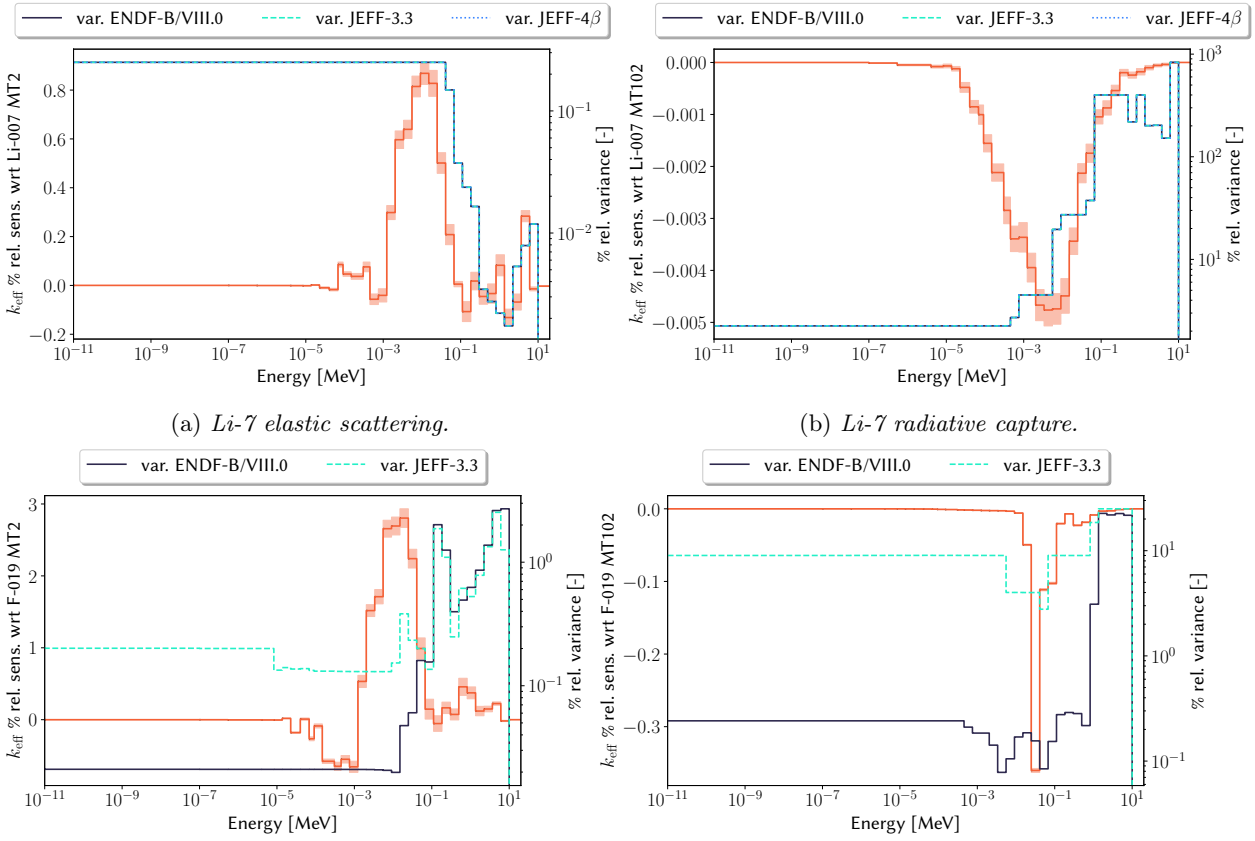

(a) *Li-7 elastic scattering.*

(b) *Li-7 radiative capture.*

(c) *F-19 elastic scattering.*

(d) *F-7 radiative capture.*

Fig. 6. *Sensitivities and relative variances for some non-fissile isotopes of interest. The shaded area indicates the* 2σ *confidence interval.*

in [34]. More accurate evaluations of these coefficients would require more latent generations, but this additional evaluation was not judged necessary for this kind of analysis, due to the small values of the sensitivities with respect to other reaction channels. All libraries present the same variance for ^{7}Li, while for ^{19}F the variance in the JEFF-3.3 library can be much larger, up to two orders of magnitude for the MT102, than the one in the ENDF-B/VIII.0. No covariance could be found in the ENDF-6 file of ^{19}F taken from JEFF-4β, probably because this library has not been officially released yet.

Figure 7 shows the MT2, MT18 (total fission) and MT102 for ^{232}Th and ^{233}U. The data for the first isotope are in perfect agreement among the various libraries, while the JEFF and ENDF/B evaluations for the variance of the cross sections of ^{233}U exhibit remarkable differences, up to three orders of magnitude for the total fission cross section. For this last case, it is important to observe that the sensitivity is around its maximum in correspondence to this large discrepancy. On the contrary, the largest sensitivity of ^{232}Th corresponds to a small value in the variance of its fission cross section, suggesting that the uncertainty due to the total fission of this isotope should have a small contribution.

The various contributions to the overall uncertainties, obtained by applying eq. (1), are analysed in figs. 8 and 9 and in tables II and III. In fig. 8, the contributions to the total uncertainty due to the location of the isotopes in the various regions of the reactor are provided for the ENDF/B-VIII.0, JEFF-3.3, and JEFF-4β libraries. As one could expect, most of the uncertainties on k_{eff} are due to the salt present in the core and in the breeding blanket, while the salt circulating in the hot and cold legs has a smaller impact. Consistently with the significant difference between the JEFF-3.3 and ENDF/B-VIII.0 covariance evaluations for ^{19}F and ^{233}U observed in fig. 7, the largest discrepancies due to the library selection can be found for these isotopes. It should be noticed that the correlation between different reactions is automatically accounted for by the presence of off-diagonal terms in the covariance matrix extracted by the ENDF file with the ERRORR module of NJOY.

Similarly, tables tables II and III provide the partial uncertainties associated with the most important MT reactions of the isotopes composing the salt. The number in parenthesis should be interpreted as $\pm$ on the last digit appearing in the table. The inspection of these tables is very instructive. First, it is easy to notice that the largest uncertainties are due to the fissile isotopes,

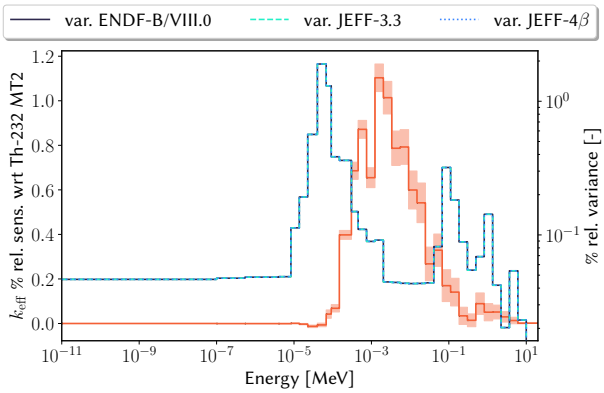

(a) *Th-232 elastic scattering.*

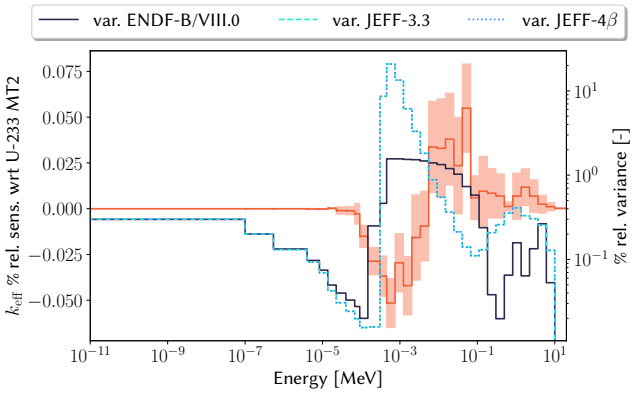

(b) *U-233 elastic scattering.*

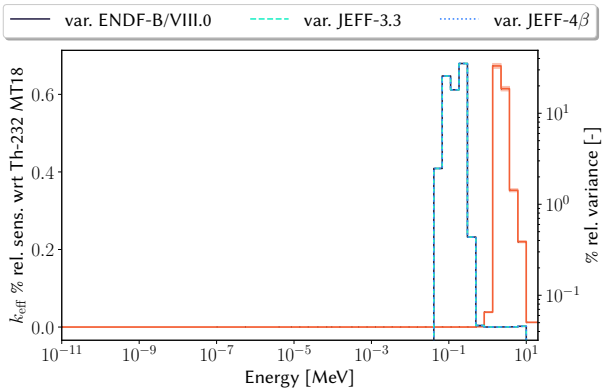

(c) *Th-232 total fission.*

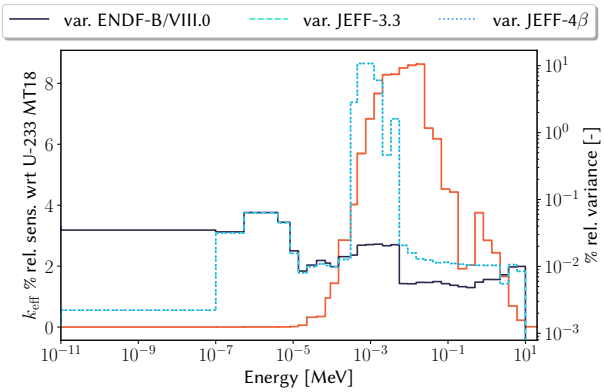

(d) *U-233 total fission.*

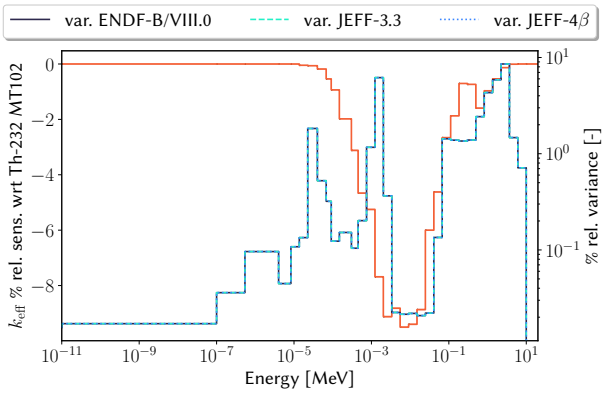

(e) *Th-232 radiative capture.*

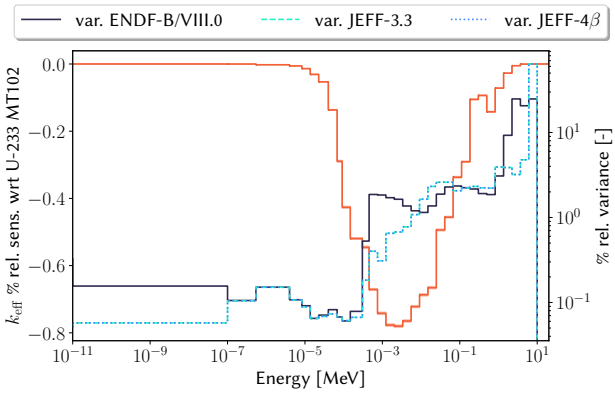

(f) *U-233 radiative capture.*

Fig. 7. *Sensitivities and relative variances for the fissile isotopes.*

TABLE II
Nuclear data uncertainties, in pcm, per MT reaction evaluated with the ENDF-B/VIII.0 library.

[pcm]	^{7}Li	^{19}F	^{232}Th	^{233}U
MT2	120(3)	109(4)	93(3)	3(3)
MT16		0.05(0)		0.5(1)
MT18			20.2(1)	327.7(2)
MT22		1.3(3)		
MT102	5.3(1)	13.0(1)	1347(2)	402.8(6)
MT107		59.6(2)		
tot.	121(3)	125(4)	1348(1)	519.4(5)

TABLE III
Nuclear data uncertainties, in pcm, per MT reaction evaluated with the JEFF-3.3 library.

[pcm]	^{7}Li	^{19}F	^{232}Th	^{233}U
MT2	120(3)	203(5)	93(3)	19(6)
MT16		0.05(0)		0.6(1)
MT18			20.2(1)	4000(5)
MT22		1.3(3)	20.2(1)	
MT102	5.3(1)	62.2(3)	1347(2)	347.8(6)
MT107		147.8(5)		
tot.	121(3)	263(4)	1348(1)	4030(6)

in particular to the radiative capture (MT102) of ^{232}Th and to the fission (MT18) and radiative capture of ^{233}U. Then, it is interesting to notice that the different covariances in the ^{233}U data are responsible for extremely large differences in the uncertainty of this isotope, which may induce about 4000 pcm on k_{eff} if the JEFF library was employed. Both the inconsistency in the data for ^{233}U and the large uncertainty due to ^{232}Th seem to demand a mandatory improvement in the data evaluation of these nuclides to safely proceed with the development of the MSFR.

Summing up all the contributions for each MT and each spatial region it is possible to estimate the most relevant contributions due to each isotope. According to the graph in fig. 9, analysing only the data for the isotopes composing the salt could be sufficient for a thorough UP study involving the reactor, thus substantially reducing the number of input parameters.

IV.B. Uncertainty analyses with TMC

The large uncertainty in k_{eff} due to the fissile isotopes and the poor statistical quality of the sensitivity profiles computed for the other integral responses suggest to adopt the TMC approach

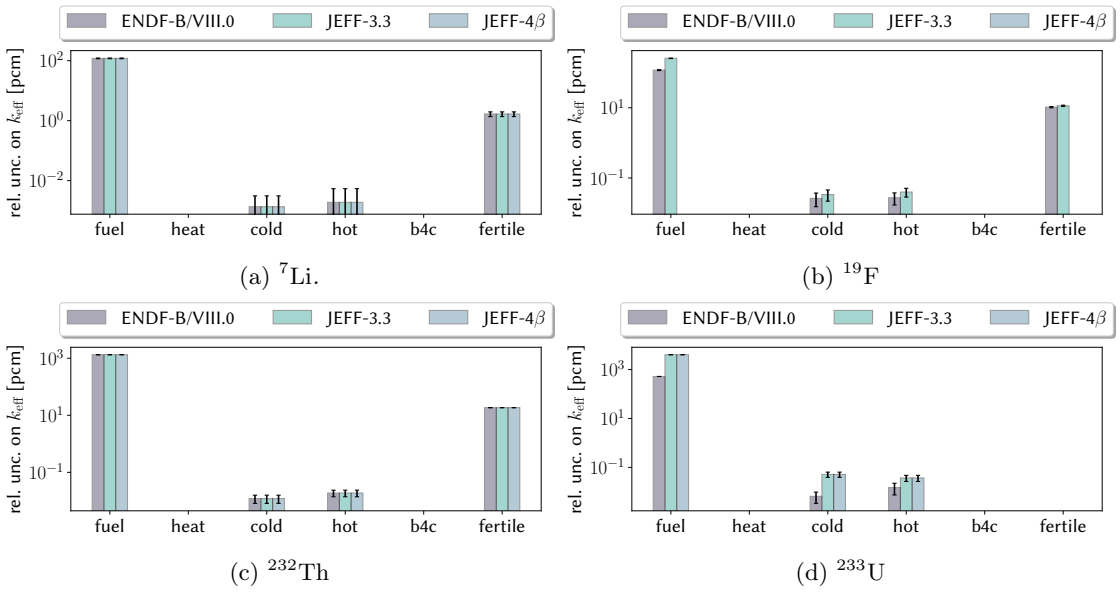

(a) ^{7}Li. (b) ^{19}F

(c) ^{232}Th (d) ^{233}U

Fig. 8. *Uncertainty contributions for each nuclide according to its spatial location in the reactor (fuel: fuel salt in the core; heat: salt in the heat exchanger; hot: salt in the hot leg; cold: salt in the cold leg; b4c: neutron shield; fertile: fertile salt in the blanket).*

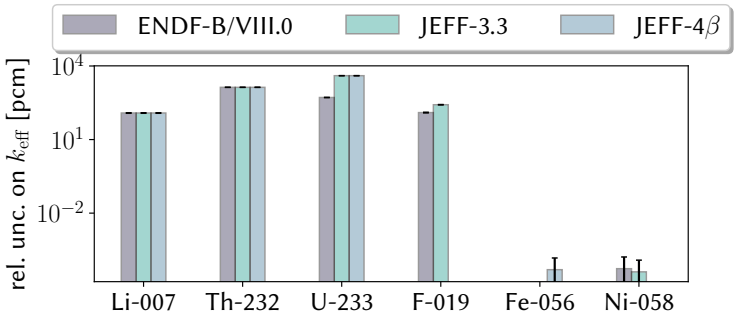

Fig. 9. *Contributions of each nuclide to the overall uncertainty on* k_{eff} .

in order to investigate also the sample distribution. Since the cost of each Serpent 2 calculation is weakly dependent on the number of output responses compared to a GPT run, also the group constants for some reactor regions have been added to the other integral responses, in view of future UP studies oriented to a multi-physics simulation framework. Each model execution was run using 60 active cycles and 20 inactive cycles, each with 10^6 neutrons and starting from an already converged fission source. The computational time required by a single simulation amounts to about 30 minutes on 24 CPUs on the same cluster used for the GPT calculation.

Figure 10 presents the convergence trends of the first and second order moments for k_{eff} and for the fast fission cross section featuring the fuel salt, obtained with 500 random cross section files for ^{233}U. The group constants are collapsed on the six-group energy grid appearing in table IV.

TABLE IV
Six-group energy grid adopted to perform the macroscopic cross section energy collapsing.

Group	Upper boundary [MeV]	Lower boundary [MeV]
1	$2.000 \cdot 10^{1}$	$2.23130 \cdot 10^{0}$
2	$2.23130 \cdot 10^{0}$	$4.97871 \cdot 10^{-1}$
3	$4.97871 \cdot 10^{-1}$	$2.47875 \cdot 10^{-2}$
4	$2.47875 \cdot 10^{-2}$	$5.53084 \cdot 10^{-3}$
5	$5.53084 \cdot 10^{-3}$	$7.48518 \cdot 10^{-4}$
6	$7.48518 \cdot 10^{-4}$	$1.000 \cdot 10^{-11}$

Each random file was generated with SANDY, perturbing the data with the information in the MF32 and MF33 sections (related to the cross sections and resonances parameters, respectively) available in the covariance matrix of the ENDF/B-VIII.0 library, scored on the ECCO-33 grid. The graphs show that both moments of the output distributions are well captured, in spite of the quite limited number of model evaluations. Figure 10(d) shows the relative standard deviation for all the six fission cross sections, while fig. 10(c) displays only the fast cross section to avoid the graph becoming too busy.

The sample distributions of some selected responses computed perturbing the ^{19}F, ^{233}U and ^{232}Th cross sections are reported in fig. 11 fig. 12 and fig. 13, respectively.

Along the diagonal of these graphs, it is possible to observe the sample distributions of the responses, namely k_{eff}, the conversion ratio CR, i.e. the number of fissile nuclei produced per each fissile nucleus consumed and the neutron lifetime l, while on the other graphs the correlations between each parameter are reported. The largest correlation can be appreciated between CR and

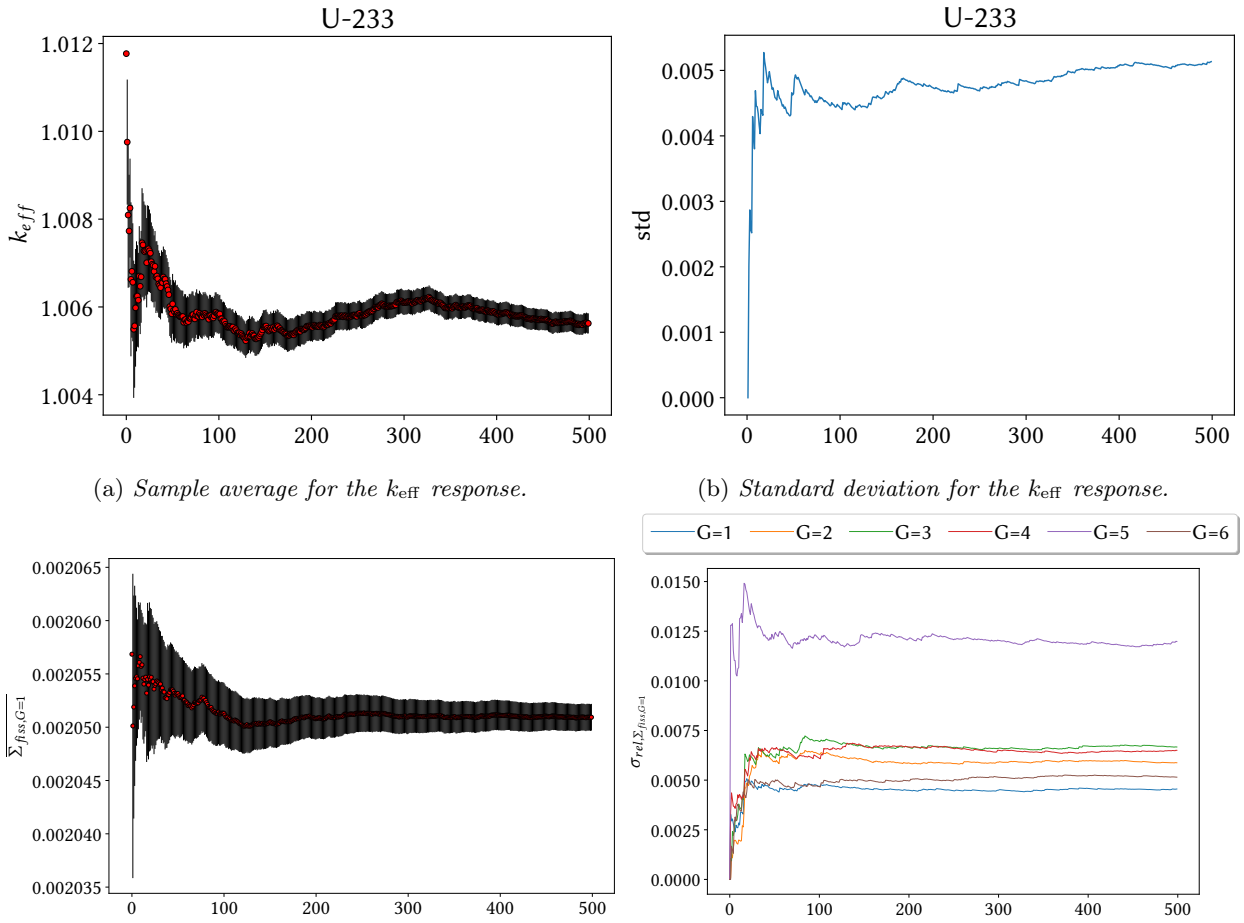

(a) *Sample average for the* k_{eff} *response.*

(b) *Standard deviation for the* k_{eff} *response.*

(c) *Sample average for the* Σ_f *response in the fast group (G=1).*

(d) *Standard deviation for the* Σ_f *response for various energy groups.*

Fig. 10. *Convergence of mean value and standard deviation of some responses of interest obtained perturbing* ^{233}U.

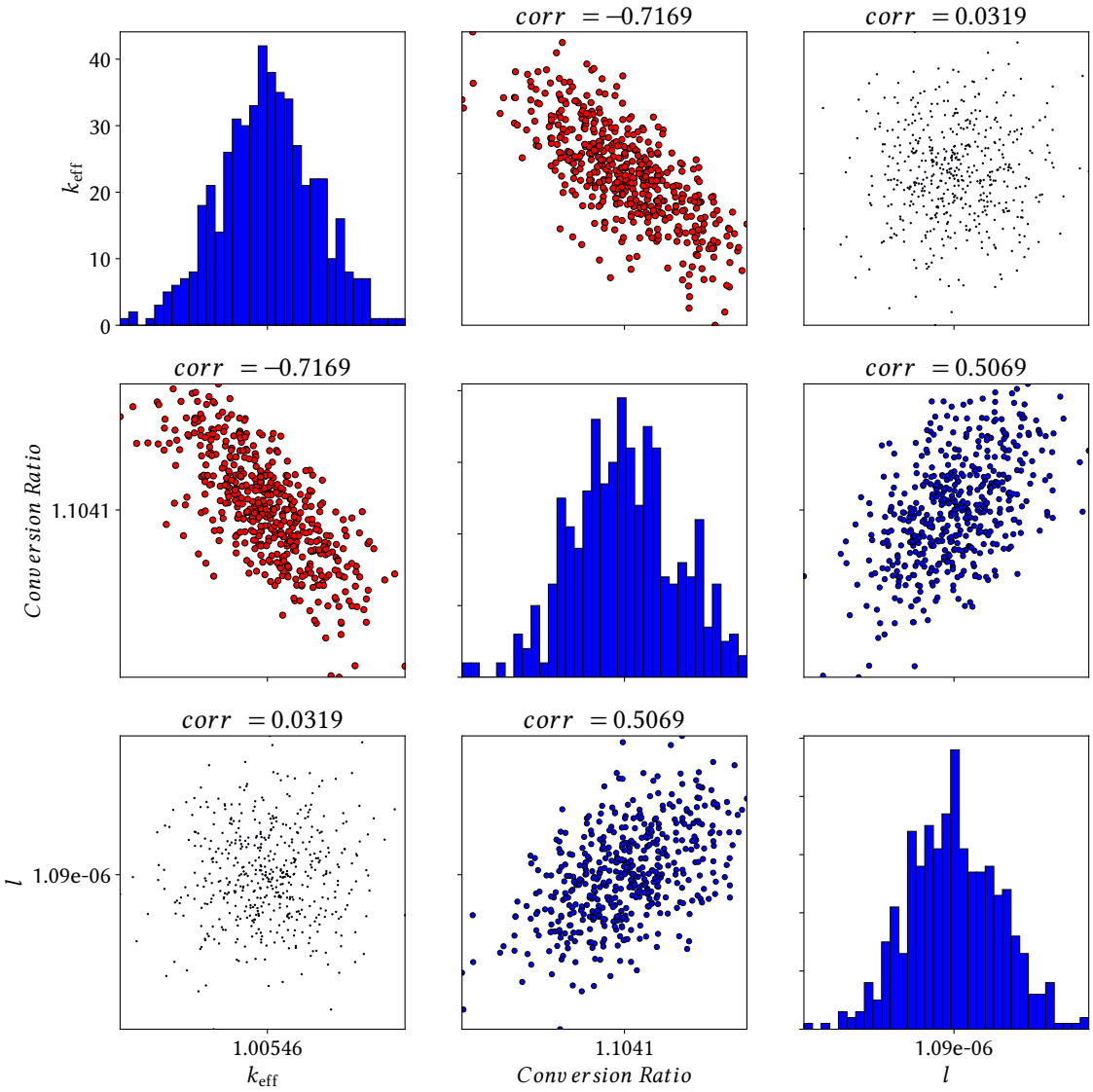

Fig. 11. *Distributions and correlation plots of some responses of interest obtained perturbing* ^{19}F. *The neutron lifetime is expressed in seconds. Larger dots correspond to stronger correlations.*

l, which are both dependent on the absorption cross section of ^{233}U, namely

$$CR = \frac{\langle 1|\Sigma_{a,^{232}\text{Th}}\Phi\rangle}{\langle 1|\Sigma_{a,^{233}\text{U}}\Phi\rangle} \tag{16}$$

and

$$l = k_{\text{eff}}\Lambda = \frac{\langle \Phi^\dagger|\frac{1}{\text{v}}\Phi\rangle}{\langle \Phi^\dagger|\hat{L}\Phi\rangle}, \tag{17}$$

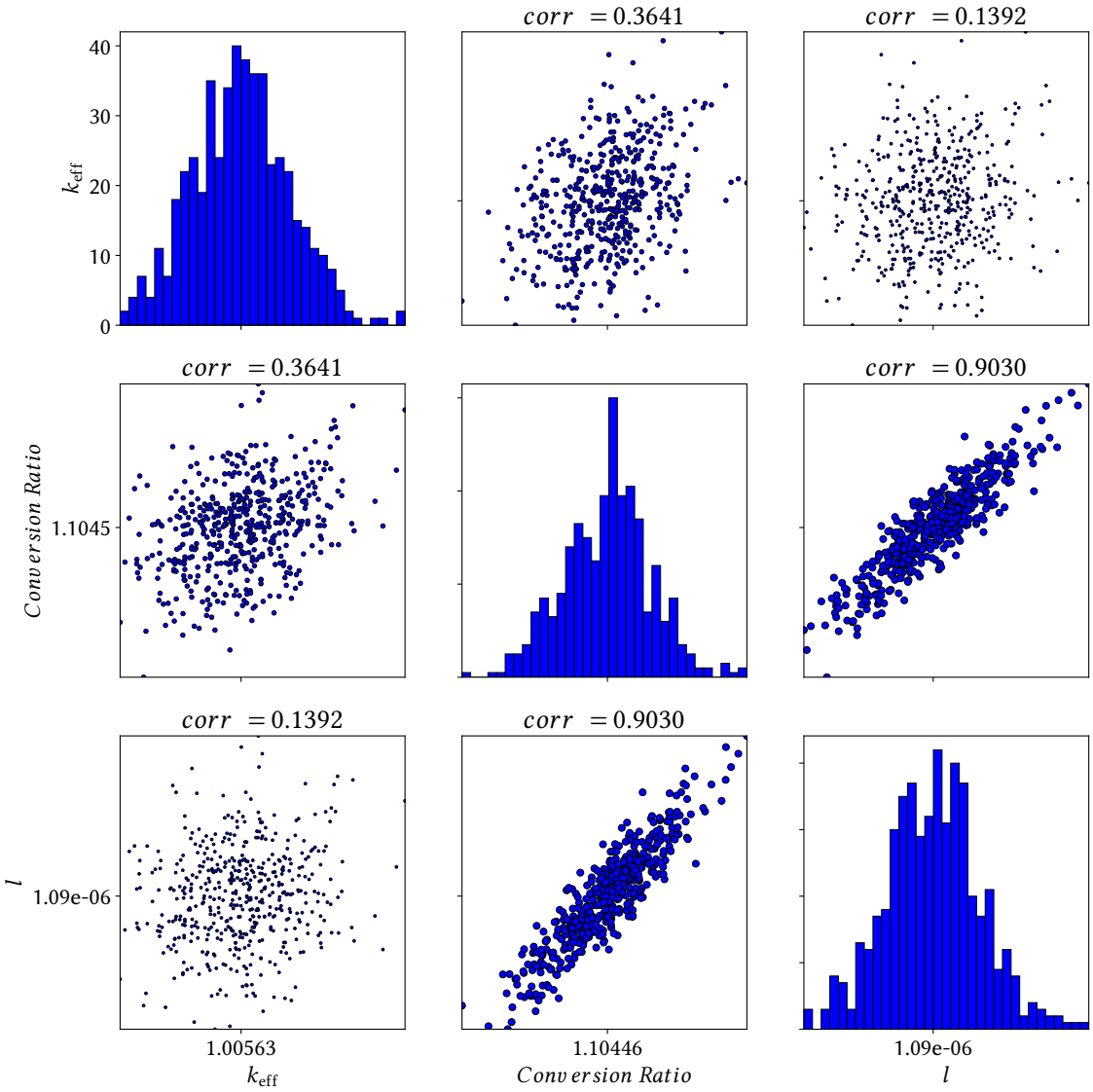

Fig. 12. *Distributions and correlation plots of some responses of interest obtained perturbing* ^{233}U. *The neutron lifetime is expressed in seconds. Larger dots correspond to stronger correlations.*

where the terms have their usual meaning. Since the leakage operator $\hat{L}$ is proportional to the absorption cross section of the system, both CR and l increase when $\Sigma_{a,^{233}\text{U}}$ decreases. The opposite behaviour can be appreciated for ^{232}Th in fig. 13, where these two parameters are negatively correlated. For the Th case, strong correlations can be appreciated also between CR and k_{eff} and between l and k_{eff}. The first dependence is due to the parasitic capture in the ^{232}Th, which increases the conversion ratio at the expenses of the neutron multiplication. While in the U case

l and k_{eff} exhibit a small correlation, perturbations in the Th cross section induce a high, positive correlation between these parameters. This behaviour is physically consistent, since both terms are inversely proportional to the absorption in the fertile isotope, which is the dominant contribution to the absorption cross section of the salt.

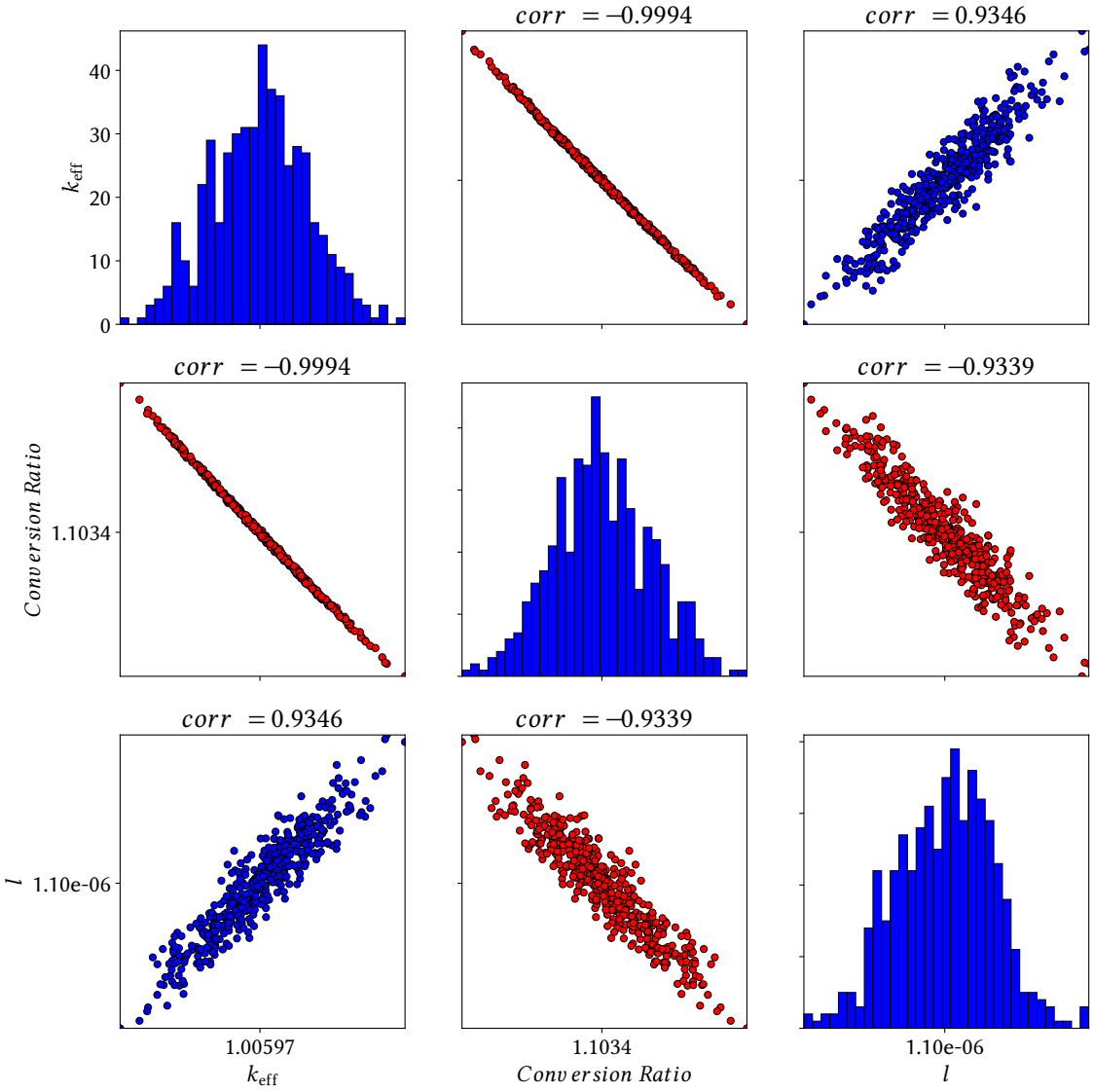

Fig. 13. *Distributions and correlation plots of some responses of interest obtained perturbing ^{232}Th. The neutron lifetime is expressed in seconds. Larger dots correspond to stronger correlations.*

Figures 14 to 16 show the sample distributions of the removal cross section, fission cross section and diffusion coefficient for the core and the blanket regions, with decreasing group energy

from left to right, for the ^{19}F, ^{233}U and ^{232}Th cases, respectively.

For each distribution, the Kolmogorov-Smirnov statistical test was performed to verify the hypothesis of having normally distributed samples. The distributions coloured in red are not recognised as normal by the test, while the ones in green may be described with a Gaussian. Since the blanket region does not contain fissile material, the indirect effect due to the perturbation in the ^{233}U data is rather small, thus justifying the small spread in the distributions and their non-normality.

Since most of the other data seems adequately described by a normal distribution, low-order techniques like the GPT or the UT seem appropriate to convey sufficiently accurate information on the response statistics.

IV.C. Uncertainty analyses with UT

In this section, the Unscented Transform is combined with the SVD in order to perform a limited number of model executions with a set of deterministic samples, i.e. the sigma points. The resulting model responses are then properly weighted to yield both the mean and the variance of the model.

As mentioned in section III.B.2, the performances of this method depend on the number of singular values adopted in the truncation of the SVD and on the shape parameter λ, which determines the spread of the sigma points and, consequently, their weights. A recent application of this UT/SVD framework to the nuclear data uncertainty propagation for a thermal water reactor using SCALE [35] showed that thanks to the strong correlation in the covariance matrices, an effective reduction could be achieved using only a few SV. The results reported in this work also suggest that the performances of the UT are weakly dependent on λ for this kind of applications.

Despite these suggestions from the literature, the application presented in this paper differs in one important aspect, related to the modelling framework. In case a deterministic model is used, the user can always distinguish, within machine precision, the variations in the output due to the variations in the input. On the contrary, when the model is stochastic, the epistemic variation may be hidden by the aleatoric one. In other words, when the $(k + \lambda)$ scaling factor is too small (e.g $k + \lambda = 3$, the value suggested in the literature for Gaussian-distributed inputs [11]), the small spread in the sigma points does not allow to distinguish the uncertainty in the response due

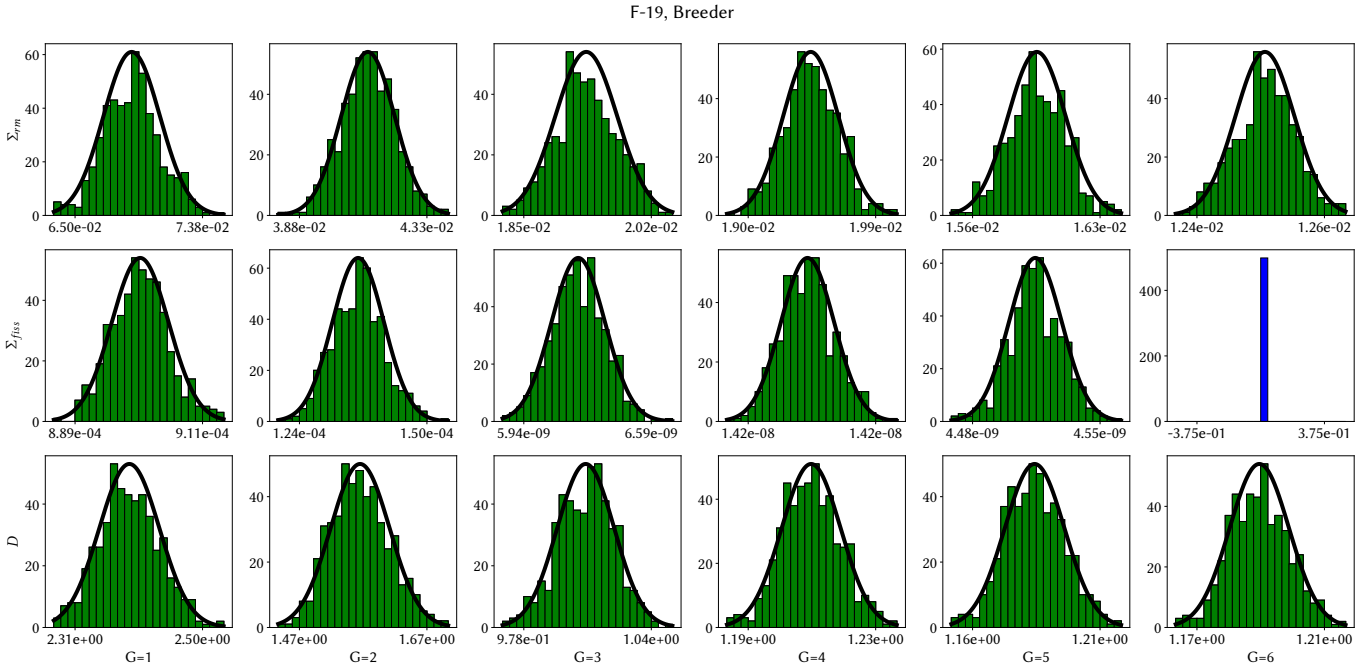

(a)

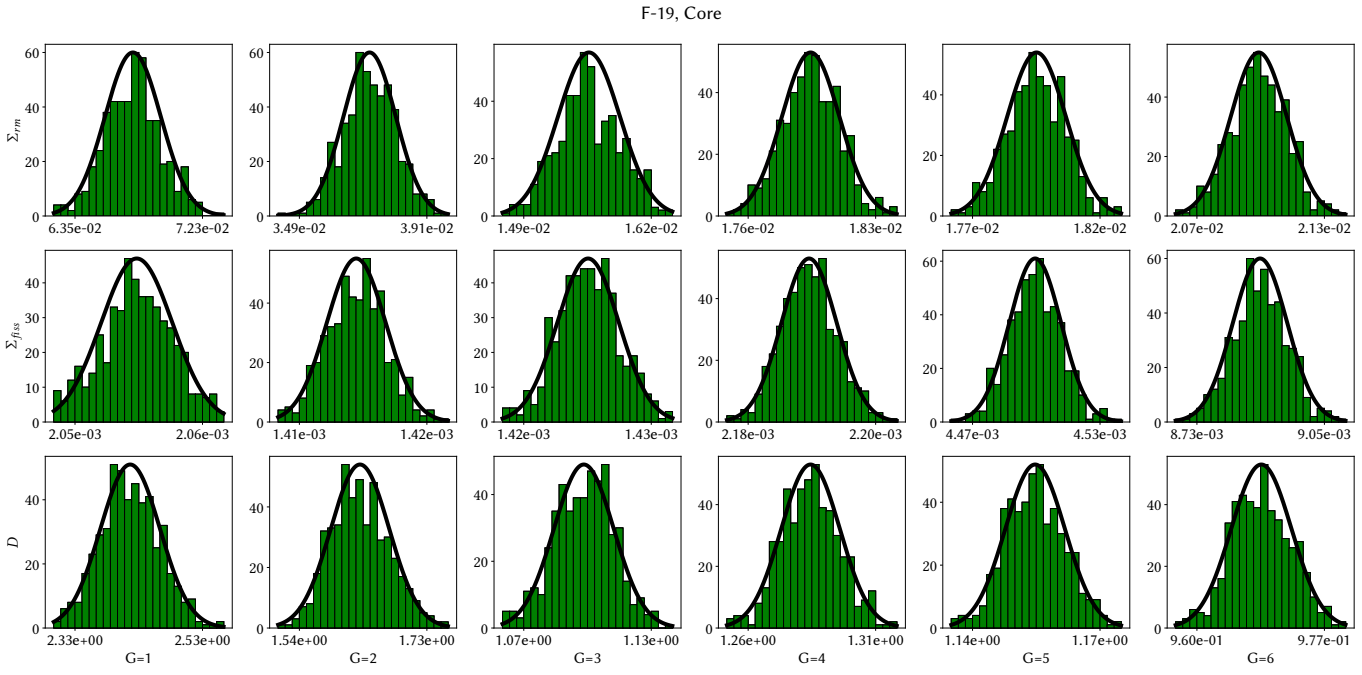

(b)

Fig. 14. *Distributions of some group constants of interest obtained perturbing ^{19}F. Color legend of the Kolmogorov-Smirnov test results: green, the test suggests a Gaussian distribution; red, the test suggests a non-Gaussian distribution.*

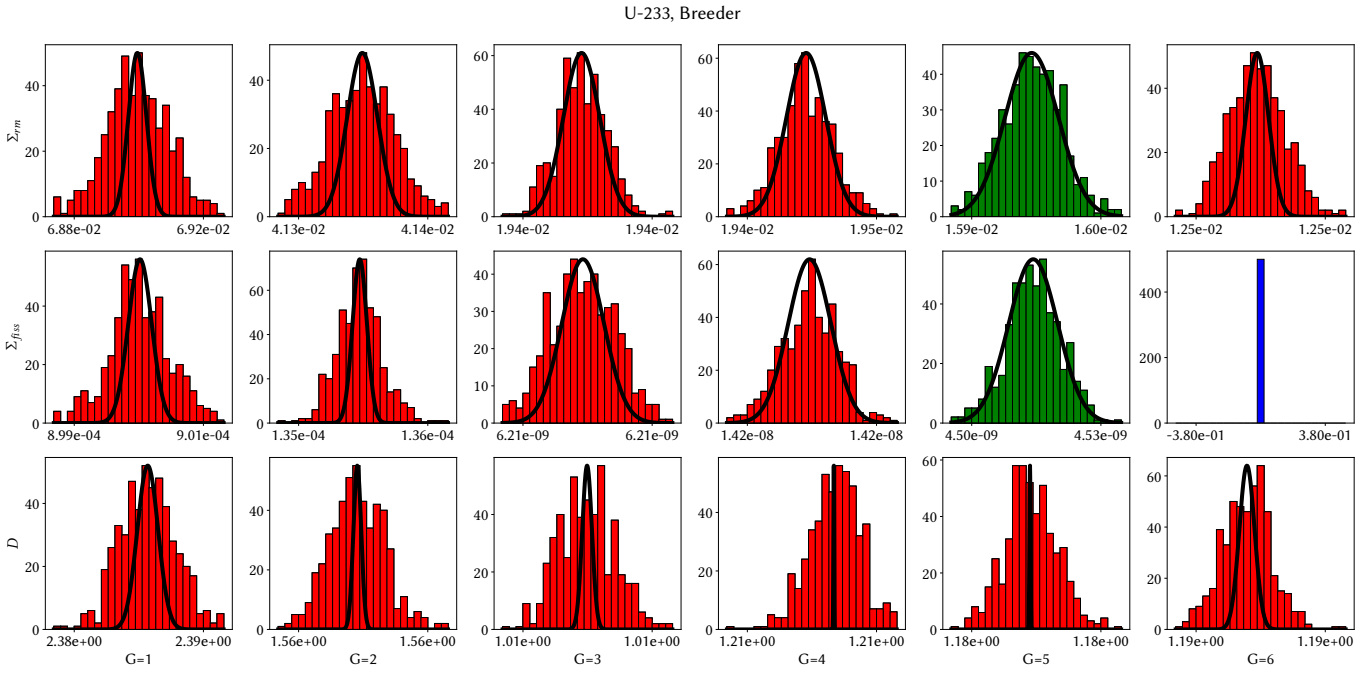

(a)

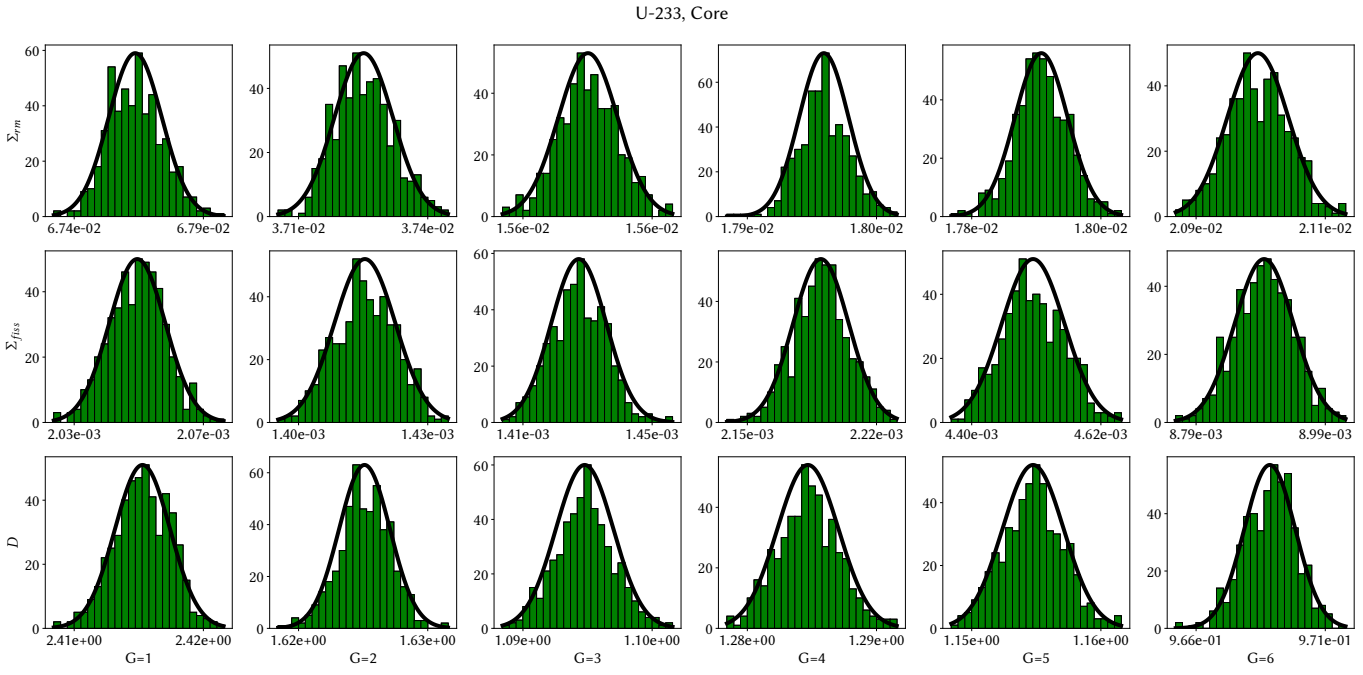

(b)

Fig. 15. *Distributions of some group constants of interest obtained perturbing* ^{233}U*. Color legend of the Kolmogorov-Smirnov test results: green, the test suggests a Gaussian distribution; red, the test suggests a non-Gaussian distribution.*

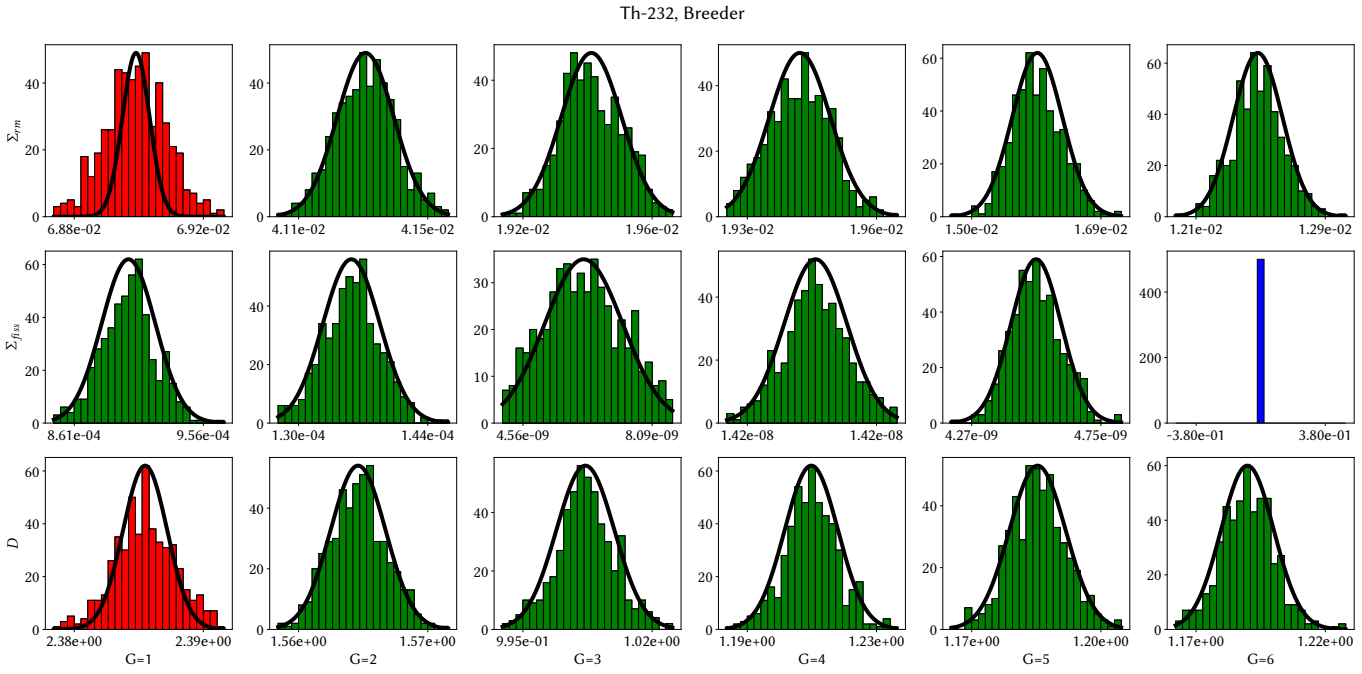

(a)

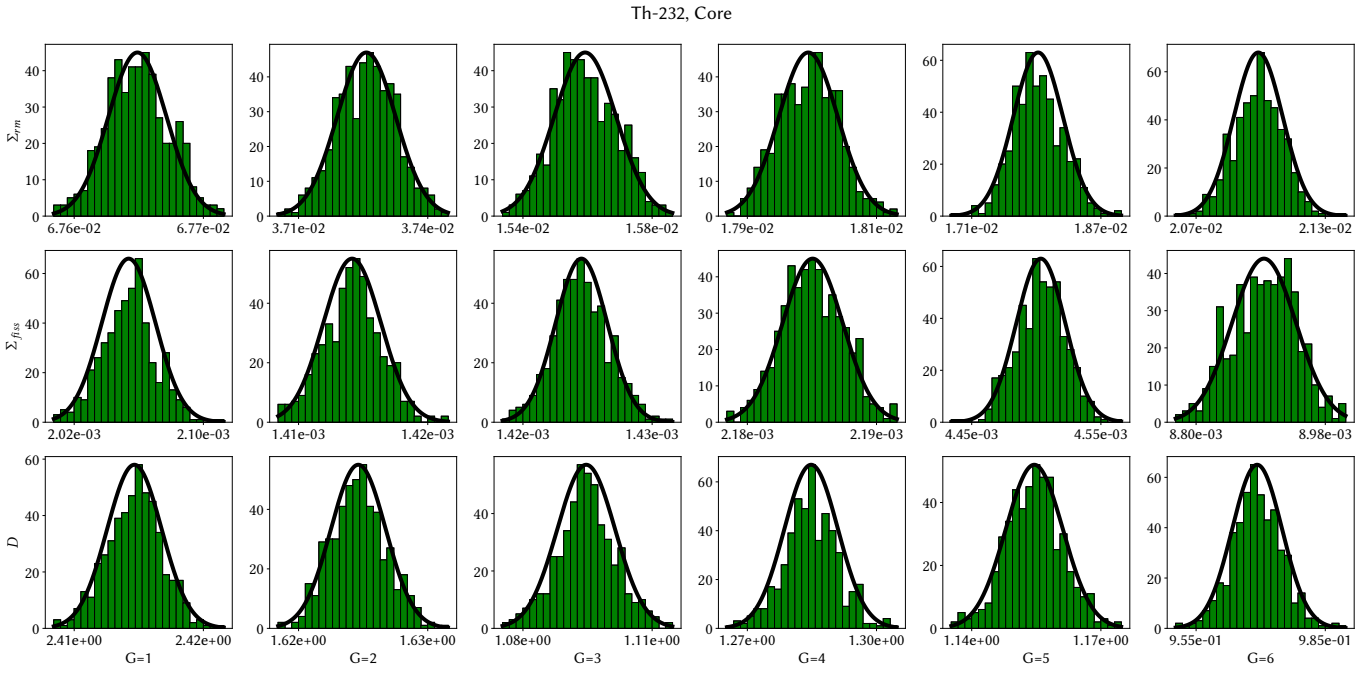

(b)

Fig. 16. *Distributions of some group constants of interest obtained perturbing* ^{232}*Th. Color legend of the Kolmogorov-Smirnov test results: green, the test suggests a Gaussian distribution; red, the test suggests a non-Gaussian distribution.*

to the data from the one due to the Monte Carlo simulation. Increasing the number of active histories in each Monte Carlo simulation to reduce the aleatoric uncertainty may not always be convenient, because of the slow convergence featuring the method. Therefore, an intuitive and easy way of avoiding this issue could be taking larger values of λ to induce larger variations in the sigma points. In this case, however, the perturbation factors in the cross sections could be so large that they could fall outside the physical limits imposed by SANDY, i.e. [0, 2]. In this case, to avoid non-physical data, SANDY would automatically "cut" the values beyond these limits, as explained in section III.B.2. Some clear examples of this condition are visible in fig. 17, which shows the energy distribution of the perturbation factors related to some sigma points. Exploiting the group-wise sensitivities computed with GPT, which are also displayed in these figures, it is possible to appreciate whether the truncation operated by SANDY involves energy groups with a large sensitivity. In the Th case, only a couple of perturbation factors are cut at relevant energies, while in the U case most of the perturbation factors fall in correspondence of large sensitivities.

To avoid this issue, which is relevant also for deterministic calculations, the GCSP method has been adopted in order to modify the values of the sigma points falling outside the acceptable range and the corresponding weights.

Tables V through to VIII summarise the mean and standard deviation of the integral parameters for the major contributors to the system uncertainty. Each model execution needed by the UT was run using 60 active cycles and 20 inactive cycles, each with 10^6 particles and starting from an already converged fission source.

In table V the uncertainties pertaining to ^{19}F are reported. The first three rows of the table show the influence of the SVD truncation by truncating the covariance matrix with 23, 47, and 77 singular values. The choice of these truncation levels can be appreciated in fig. 18, where they are indicated as vertical dashed lines dividing the SV sequence. Considering that the number of model execution scales like $2t + 1$, where t is the number of SV, this parameter is relevant for the computational performances of the model. The estimates of the standard deviation for k_{eff} present some small deviations with respect to the TMC value, which is assumed here as a reference, but these differences could be acceptable if the objective of the UP is to have a rough idea of the various contributions to the overall uncertainty. The table also reports some calculations carried out with a fixed number of SV but different values of the shape parameter λ. When $\lambda = 0.5$,

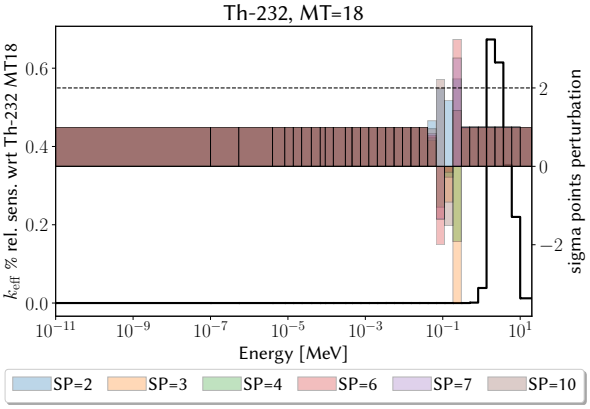

(a) *Th-232 total fission.*

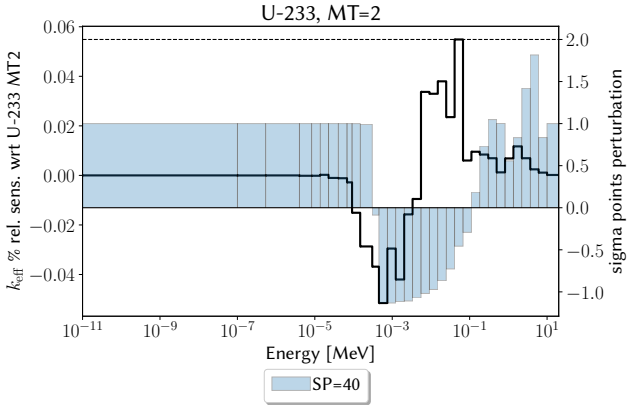

(b) *U-233 elastic scattering.*

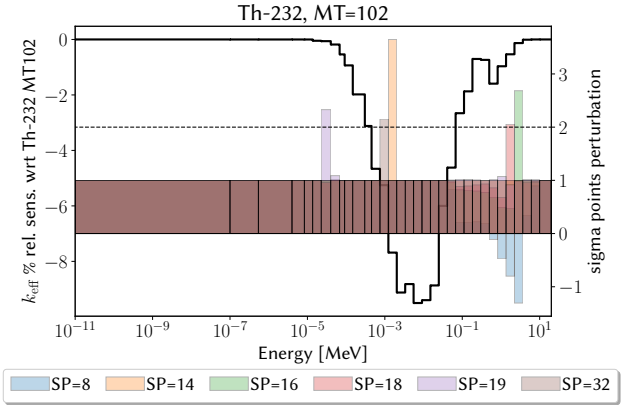

(c) *Th-232 radiative capture.*

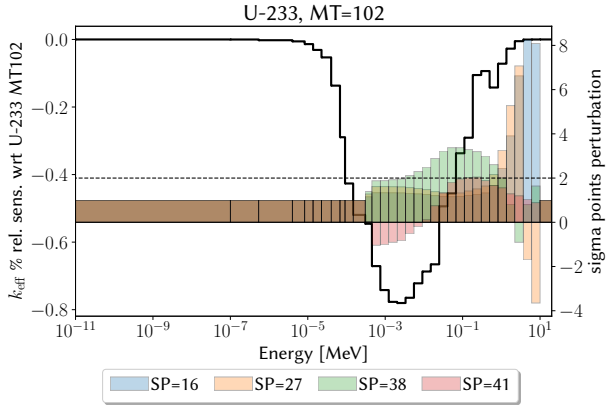

(d) *U-233 radiative capture.*

Fig. 17. *Sensitivities and sigma points (SP) outside the range (0, 2) for the fissile isotopes.*

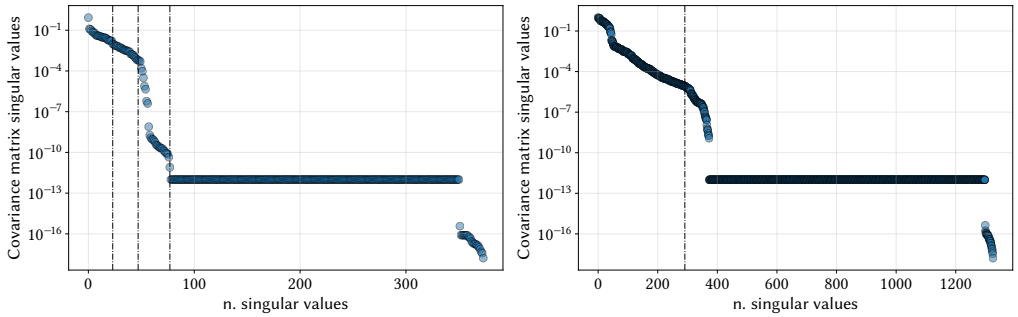

(a) *F-19.* (b) *U-233.*

Fig. 18. *Profile of the singular values of F-19 and U-233, scoring the covariance matrices on the ECCO-33 group structure.*

the spread in the sigma points leads to some truncations in the perturbation factors, which are responsible for the larger discrepancy in the standard deviation, while when $\lambda = -74$ the spread in the sigma points is reduced but the statistical noise of each model execution increases. As a consequence, the statistical uncertainty on the standard deviation gets larger. When the GCSP is used, the sigma points are not approximated, yielding a larger uncertainty that is closer to the reference value obtained with TMC.

TABLE V
Nuclear data uncertainty of ^{19}F with ENDF-B/VIII.0 library.

	k_{eff} [−]	std. [pcm]	CR [−]	std. [pcm]	l [s]	std. [pcm]
TMC, 33-G	1.00546	151(13)	1.10410	211(16)	1.0937e-06	0.00048(4)
UT, 33-G, $\lambda = 0.5$, 23 SV	1.00547(3)	125(3)	1.10416(13)	193(13)	1.0939(6)e-6	0.00047(6)
UT, 33-G, $\lambda = 0.5$, 47 SV	1.00543(2)	139(2)	1.10419(9)	179(9)	1.0940(4)e-6	0.00046(4)
UT, 33-G, $\lambda = 0.5$, 77 SV	1.00541(1)	135(2)	1.10424(2)	161(7)	1.0938(1)e-6	0.00044(3)
UT, 33-G, $\lambda = -74$, 77 SV	1.00573(179)	147(39)	1.10723(78)	–	1.0891(341)e-6	–
UT_{GCSP}, 33-G, $\lambda = 0.5$, 77 SV	1.00541(11)	151(2)	1.10408(42)	220(13)	1.09344(199)e-6	0.00051(5)
GPT, 33-G	1.00544(2)	125 (4)	1.10450(20)	–	1.09403(70)E-06	–

Table VI presents a comparison between UT and GPT for ^{7}Li, showing a good agreement in virtue of the absence of perturbation factors outside the range for the elastic scattering (MT2),

TABLE VI
Nuclear data uncertainty of ^{7}Li with ENDF-B/VIII.0 library.

	k_{eff} [−]	std. [pcm]	CR [−]	std. [pcm]	l [s]	std. [pcm]
UT, 33-G, $\lambda = 0.5$, 54 SV	1.00543(2)	124(1)	1.10429(9)	209(8)	1.0942(4)e-6	0.00045(4)
GPT, 33-G	1.00544	121(3)	1.10450(20)	–	1.09403(70)E-06	–

which has the highest contribution to the k_{eff} uncertainty (see table II). The last two tables, table VII and table VIII, are related to the fissile isotopes. In both cases, the agreement between TMC, GPT and UT with the CGSP correction is good, especially for the ^{233}U case. When the CGSP correction is not employed, the uncertainties with respect to the reference are heavily underestimated, consistently with the behaviour observed in fig. 17. A possible cause for the discrepancy between GPT and TMC for the Th case could be the fact that also the TMC samples, which are sampled according to a multi-variate normal distribution by SANDY, may present some truncation in the perturbation factors. Another source of discrepancy could be due to the first-order accuracy of the sandwich rule, which could be not precise enough when the uncertainty in the data is large, as in this case.

TABLE VII
Nuclear data uncertainty of ^{233}U with ENDF-B/VIII.0 library.

	k_{eff} [−]	std. [pcm]	CR [−]	std. [pcm]	l [s]	std. [pcm]
TMC, 33-G	1.00563	513(38)	1.10445	1084(99)	1.09424e-06	0.00072(6)
UT, 33-G, $\lambda = 0.5$, 291 SV	1.00541(1)	441(2)	1.10437(4)	846(4)	1.0942(2)e-6	0.00063(2)
UT_{GCSP}, 33-G, $\lambda = 0.5$, 291 SV	1.00497(122)	524(12)	1.10435(482)	1065(10)	1.09628(2288)e-6	0.00078(6)
GPT, 33-G	1.00544	519.4(5)	1.10450(20)	–	1.09403(70)E-06	–

V. CONCLUSIONS

In this paper, an uncertainty propagation study concerning the Molten Salt Fast Reactor under design in the frame of the SAMOFAR and SAMOSAFER European projects has been carried out, focusing on the impact of the nuclear data uncertainties featuring the isotopes in the

TABLE VIII
Nuclear data uncertainty of ^{232}Th with ENDF-B/VIII.0 library.

	k_{eff} [−]	std. [pcm]	CR [−]	std. [pcm]	l [s]	std. [pcm]
TMC, 33-G	1.00608	1284(94)	1.10318	2900(213)	1.09519e-6	0.00192(16)
UT, 33-G, $\lambda = 0.5$, 113 SV	1.00566(1)	829(1)	1.10403(6)	1865(6)	1.09450(27)e-6	0.00118(3)
UT_{GCSP}, 33-G, $\lambda = 0.5$, 113 SV	1.00609(76)	1379(5)	1.10316(303)	3089(18)	1.09628(1423)e-6	0.00198(16)
GPT, 33-G	1.00544	1348(1)	1.10450(20)	–	1.09403(70)E-06	–

salt on some relevant integral parameters, like k_{eff}, l and CR.

In the first part of the paper, some best estimate calculations are performed with the Serpent 2 Monte Carlo code using different nuclear data libraries. This analysis has revealed that the choice of the library has a dramatic impact on the final responses, suggesting that the data evaluations for the main isotopes constituting the reactor should be made consistent.

Then, some standard techniques are applied to analyse more in detail the various contributions to the overall uncertainty. First, the Monte Carlo version of the GPT is applied to estimate the sensitivity coefficients of the nuclides composing the salt with respect to k_{eff}. These coefficients are then employed in the sandwich rule to provide a first-order estimate of the uncertainties and their components, analysing the role played by the various isotopes and by the various reaction channels. In this case, it has been noticed that there are very large discrepancies in the covariance matrices of ^{233}U between the JEFF-3.3 and the ENDF/B-VIII.0 libraries, which are responsible for significant differences in the contribution of this isotope to the total uncertainty.

Afterwards, the direct sampling TMC method is applied to get the sample distributions of some interesting output responses such as group constants. This analysis showed that the hypothesis of normally distributed responses seems acceptable for most output parameters, except for some responses featured by a small variance.

Then, the uncertainties in the integral responses previously analysed with the GPT and TMC approaches are evaluated with the UT method, which is applied here to a stochastic model, differently with respect to the other applications available in the literature. Due to the peculiarities of the stochastic simulation framework and to the constraints on the perturbations applied to the nuclear data, an alternative method for the generation of the UT samples is adopted, obtaining

fairly good results compared to the other methods. This application seems to confirm that UT is a computationally efficient technique also for a stochastic model and that could replace the more expensive TMC for systematic uncertainty propagation studies. This statement is justified by the fact that the time required by each model evaluation is the same for both TMC and UT, but the number of model evaluations needed by UT is in general much smaller than the one required by TMC.

At last, the results of the uncertainty propagation study presented and discussed in this work allow to make some final remarks on the clear need for better data evaluations for the nuclides constituting the circulating salt for an effective deployment of the MSFR technology.

DATA AVAILABILITY

The complete datasets and scripts employed to pre- and post-process the calculations presented in this paper are available in the open access Zenodo repository 10.5281/zenodo.4540785.

ACKNOWLEDGMENTS

Computational resources were provided by HPC@POLITO, a project of Academic Computing within the Department of Control and Computer Engineering at Politecnico di Torino (http://www.hpc.polito.it).

The authors are also grateful to Dr. Stefano Lorenzi and his colleagues of the Nuclear Reactors Group in Politecnico di Milano for having provided the Serpent 2 model of the MSFR during the SAMOFAR project.

REFERENCES

[1] G. Locatelli, M. Mancini, and N. Todeschini. "Generation IV nuclear reactors: Current status and future prospects". In: *Energy Policy* 61 (2013), pages 1503–1520 (cited on page 3).

[2] M. Tiberga, R. G. G. de Oliveira, E. Cervi, J. A. Blanco, S. Lorenzi, M. Aufiero, D. Lathouwers, and P. Rubiolo. "Results from a multi-physics numerical benchmark for codes dedicated to molten salt fast reactors". In: *Annals of Nuclear Energy* 142 (2020), page 107428 (cited on page 3).

[3] M. Aufiero, M. Fratoni, and P. Rubiolo. "Monte Carlo/CFD coupling for accurate modeling of the delayed neutron precursors and compressibility effects in molten salt reactors". In: *Transactions of the American Nuclear Society* 116 (2017) (cited on page 3).

[4] M. Herman, A. Trkov, et al. *ENDF-6 formats manual*. Technical report BNL-90365-2009 Rev.1. 2010 (cited on page 4).

[5] R. Bellman. "Dynamic Programming". Rand Corporation research study. Princeton University Press, 1957 (cited on page 4).

[6] G. Rimpault, D. Plisson, J. Tommasi, R. Jacqmin, D. Verrier, and D. Biron. "The ERANOS Code and Data System for Fast Reactor Neutronic Analyses". In: *Proceedings of the PHYSOR conference 2002*. 2002 (cited on page 4).

[7] M. Santanoceto, M. Tiberga, Z. Perkó, S. Dulla, and D. Lathouwers. "Uncertainty quantification in steady state simulations of a molten salt system using polynomial chaos expansion analysis". In: *EPJ Web of Conferences*. Volume 247. EDP Sciences. 2021, page 15008 (cited on page 4).

[8] D. G. Cacuci. "Sensitivity & Uncertainty Analysis, Volume I: Theory". Chapman & Hall/CRC, New York, 2003, page 285 (cited on pages 4, 10).

[9] M. Aufiero, A. Bidaud, M. Hursin, J. Leppänen, G. Palmiotti, S. Pelloni, and P. Rubiolo. "A collision history-based approach to sensitivity/perturbation calculations in the continuous energy Monte Carlo code SERPENT". In: *Annals of Nuclear Energy* 85 (2015), pages 245–258 (cited on pages 4, 10).

[10] A. Koning and D. Rochman. "Towards sustainable nuclear energy: Putting nuclear physics to work". In: *Annals of Nuclear Energy* 35 (11 2008), pages 2024–2030 (cited on pages 5, 11).

[11] S. J. Julier and J. K. Uhlmann. "New extension of the Kalman filter to nonlinear systems". In: *Signal Processing, Sensor Fusion, and Target Recognition VI*. Edited by I. Kadar. Volume 3068. International Society for Optics and Photonics. SPIE, 1997, pages 182–193 (cited on pages 5, 12, 28).

[12] A. Sharma, A. Gandhi, and A. Kumar. "Estimation of optical model parameters and their correlation matrix using Unscented Transform Kalman Filter technique". In: *Physics Letters B* 815 (2021), page 136179 (cited on page 5).

[13] A. Sharma, A. Gandhi, and A. Kumar. "Deterministic sampling approach for the propagation of uncertainties in nuclear reaction models". In: *Physical Review C* 106.4 (2022), page L041601 (cited on page 5).

[14] Y. Fukui, T. Endo, and A. Yamamoto. "Nuclear data adjustment using a deterministic sampling method with unscented transformation". In: *Journal of Nuclear Science and Technology* (2022), pages 1–13 (cited on page 5).

[15] N. Abrate, M. Aufiero, S. Dulla, and L. Fiorito. "Nuclear Data Uncertainty Quantification in Molten Salt Reactors with XGPT". In: *Proceedings of the ANS International Conference M&C2019*. Portland, OR, 2019 (cited on pages 6, 10).

[16] N. Abrate. `https://github.com/nicoloabrate/ndl`. 2021 (cited on page 7).

[17] R. Macfarlane, D. W. Muir, R. M. Boicourt, A. C. Kahler III, and J. L. Conlin. "The NJOY Nuclear Data Processing System, Version 2016". In: (Jan. 2017) (cited on page 7).

[18] Los Alamos National Laboratory. `https://github.com/njoy`. 2016 (cited on page 7).

[19] A. Gandini, M. Salvatores, and I. D. Bono. "Sensitivity Study of Fast Reactors Using Generalized Perturbation Techniques". In: *Fast Reactor Physics Vol. I. Proceedings of a Symposium on Fast Reactor Physics and Related Safety Problems*. 1968 (cited on page 9).

[20] A. Gandini and M. Salvatores. "Effects of Plutonium-239 Alpha Uncertainties on some Significant Integral Quantities of Fast Reactors". In: *Nuclear Science and Engineering* 41.3 (1970), pages 452–455 (cited on page 9).

[21] M. Aufiero, M. Martin, and M. Fratoni. "XGPT: Extending Monte Carlo Generalized Perturbation Theory capabilities to continuous-energy sensitivity functions". In: *Annals of Nuclear Energy* 96 (2016), pages 295–306 (cited on page 10).

[22] N. Abrate, S. Dulla, and P. Ravetto. "Generalized perturbation techniques for uncertainty quantification in lead-cooled fast reactors". In: *Annals of Nuclear Energy* 164 (2021), page 108623 (cited on pages 10, 17).

[23] L. Fiorito, G. Žerovnik, A. Stankovskiy, G. Van den Eynde, and P. Labeau. "Nuclear data uncertainty propagation to integral responses using SANDY". In: *Annals of Nuclear Energy* 101 (2017), pages 359–366 (cited on page 11).

[24] D. Rochman, S. van der Marck, A. Koning, H. Sjöstrand, and W. Zwermann. "Uncertainty Propagation with Fast Monte Carlo Techniques". In: *Nuclear Data Sheets* 118 (2014), pages 367–369 (cited on page 11).

[25] W. Zwermann, B. Krzykacz-Hausmann, L. Gallner, M. Klein, A. Pautz, and K. Velkov. "Aleatoric and epistemic uncertainties in sampling based nuclear data uncertainty and sensitivity analyses". In: Proc. of the International Topical Meeting on Advances in Reactor Physics (PHYSOR '12), Knoxville, TN, USA, April 15–20, 2012, on CD-ROM. 2012 (cited on page 11).

[26] A. Aimetta, N. Abrate, S. Dulla, and A. Froio. "A Nonintrusive Nuclear Data Uncertainty Propagation Study for the ARC Fusion Reactor Design". In: *Nuclear Science and Engineering* (2023) (cited on page 11).

[27] B. Foad, A. Yamamoto, and T. Endo. "Efficient uncertainty quantification for PWR during LOCA using unscented transform with singular value decomposition". In: *Annals of Nuclear Energy* 141 (2020), page 107341 (cited on page 12).

[28] S. Volkwein. "Model reduction using proper orthogonal decomposition". In: *Lecture notes, Institute of Mathematics and Scientific Computing, University of Graz. see http://www. uni-graz. at/imawww/volkwein/POD. pdf* 1025 (2011) (cited on page 12).

[29] K. Nielsen, C. Svahn, H. Rodriguez-Deniz, and G. Hendeby. "UKF Parameter Tuning for Local Variation Smoothing". In: *2021 IEEE International Conference on Multisensor Fusion and Integration for Intelligent Systems (MFI)*. 2021, pages 1–8 (cited on page 13).

[30] S. Seabold and J. Perktold. "statsmodels: Econometric and statistical modeling with python". In: *9th Python in Science Conference*. 2010 (cited on page 13).

[31] R. Borsdorf, N. J. Higham, and M. Raydan. "Computing a Nearest Correlation Matrix with Factor Structure". In: *SIAM Journal on Matrix Analysis and Applications* 31 (2010), pages 2603–2622 (cited on page 13).

[32] D. Li and Y. Wang. "Constrained unscented Kalman filter for parameter identification of structural systems". In: *Structural Control and Health Monitoring* 29.4 (2022), e2908 (cited on page 15).

[33] A. E. Johnson, D. Kotlyar, S. Terlizzi, and G. Ridley. "serpentTools: A Python Package for Expediting Analysis with Serpent". In: *Nuclear Science and Engineering* 194.11 (2020), pages 1016–1024 (cited on page 17).

[34] M. Aufiero, M. Martin, M. Fratoni, E. Fridman, S. Lorenzi, et al. "Analysis of the coolant density reactivity coefficient in LFRs and SFRs via Monte Carlo perturbation/sensitivity". In: *Proceedings of the PHYSOR conference 2016*. 2016 (cited on page 19).

[35] B. Foad and D. R. Novog. "Implementation and testing of unscented transformation and low rank approximation to enhance SCALE code uncertainty calculations". In: *Annals of Nuclear Energy* 167 (2022), page 108816 (cited on page 28).